The Dynamics of the Spectra of the Periods of major indices of Solar and Geomagnetic Activity on the various phases of the Solar cycles.

«Solar Influences on the Magnetosphere, Ionosphere and Atmosphere»

Primorsko, Bulgaria, 3 ÷ 7 June 2019

Ryabov M.I, Sukharev A.L, Sobitnyak L.I., Komendant V.G.
Odessa Observatory URAN-4, Radio Astronomical Institute NAS, Ukraine

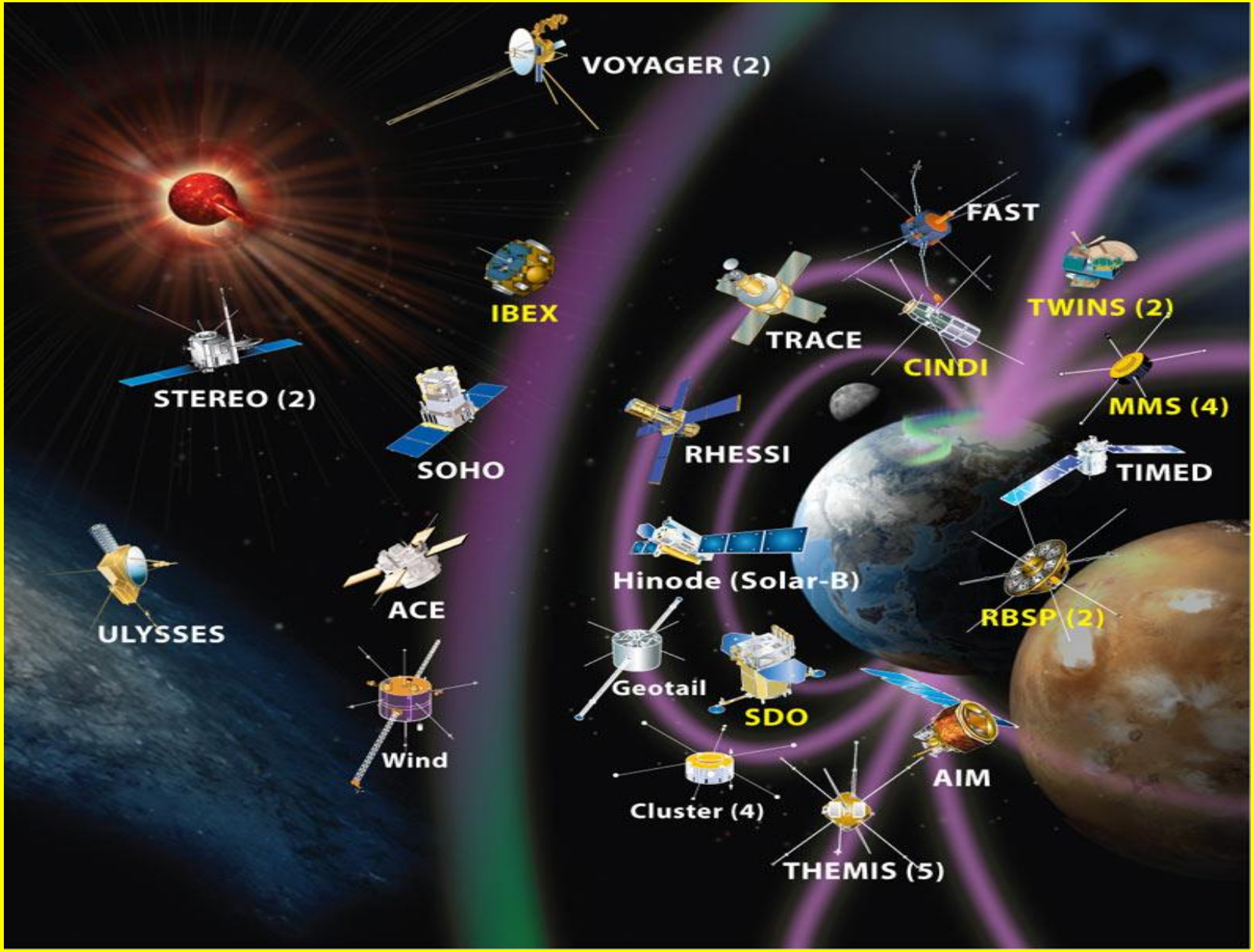
VOYAGER (2)
IBEX
STEREO (2)
SOHO
ULYSSES
ACE
Wind
FAST
TRACE
CINDI
TWINS (2)
MMS (4)
RHESSI
TIMED
Hinode (Solar-B)
RBSP (2)
Geotail
SDO
AIM
Cluster (4)
THEMIS (5)

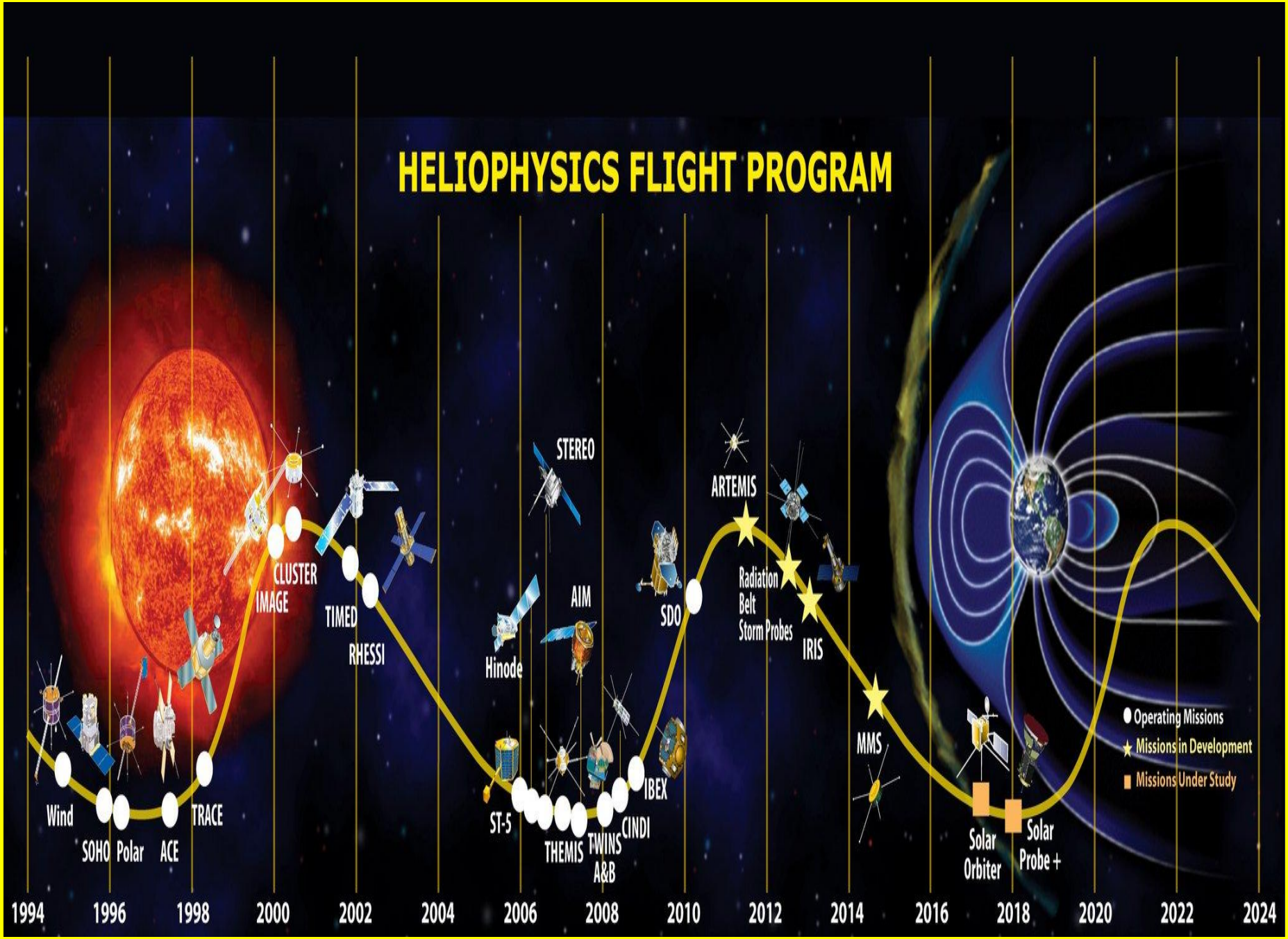
HELIOPHYSICS FLIGHT PROGRAM
Wind
SOHO
Polar
ACE
TRACE
CLUSTER
IMAGE
TIMED
RHESSI
STEREO
Hinode
AIM
ST-5
THEMIS
TWINS A&B
CINDI
IBEX
SDO
ARTEMIS
Radiation Belt Storm Probes
IRIS
MMS
Solar Orbiter
Solar Probe +
Operating Missions
Missions in Development
Missions Under Study
1994
1996
1998
2000
2002
2004
2006
2008
2010
2012
2014
2016
2018
2020
2022
2024

Physical processes of forming solar activity

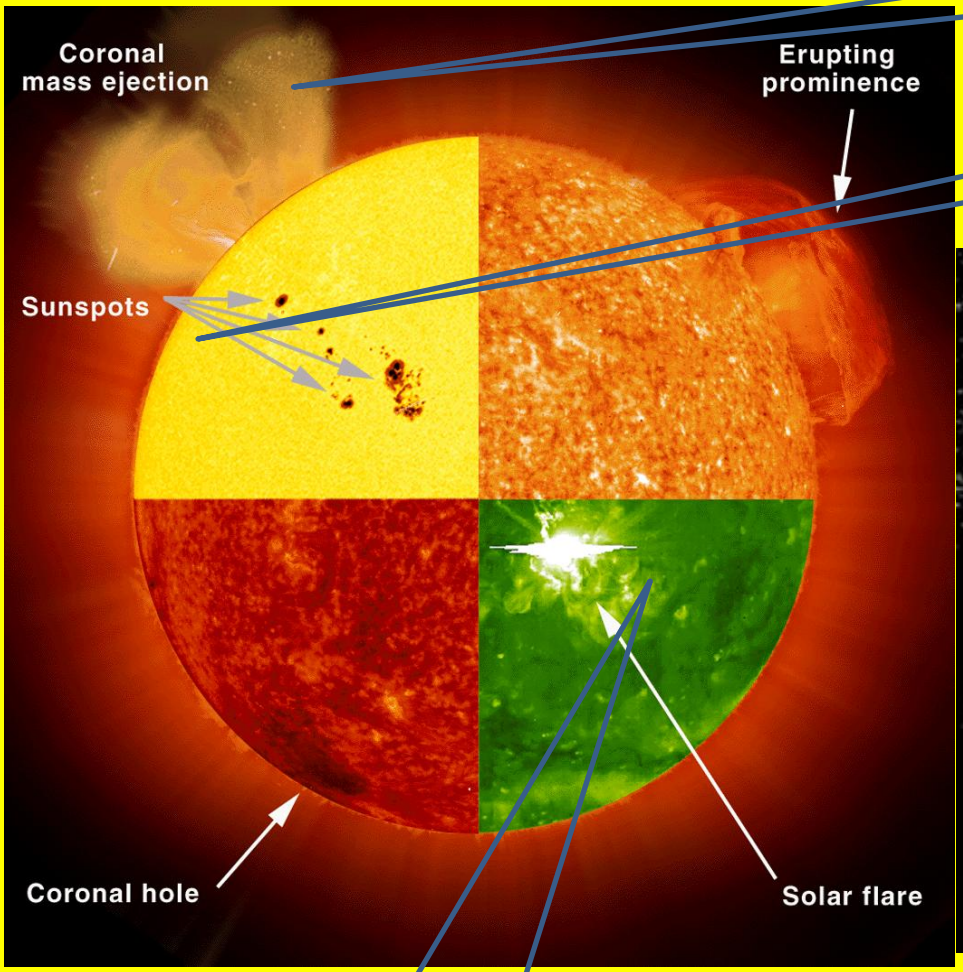

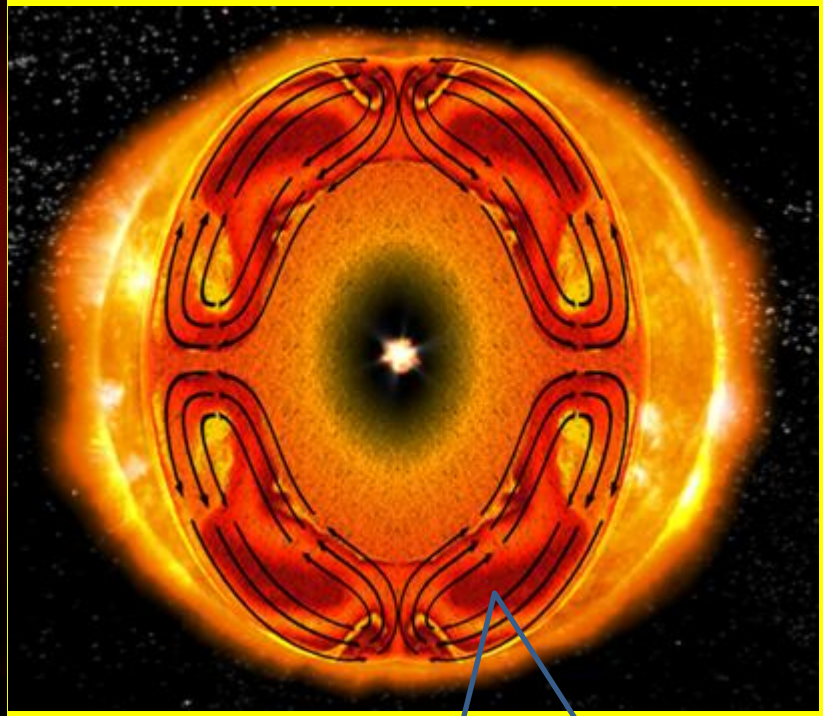

Solar corona

Photospere

Chromosphere

Convective zone

Wave and particle manifestations of solar activity

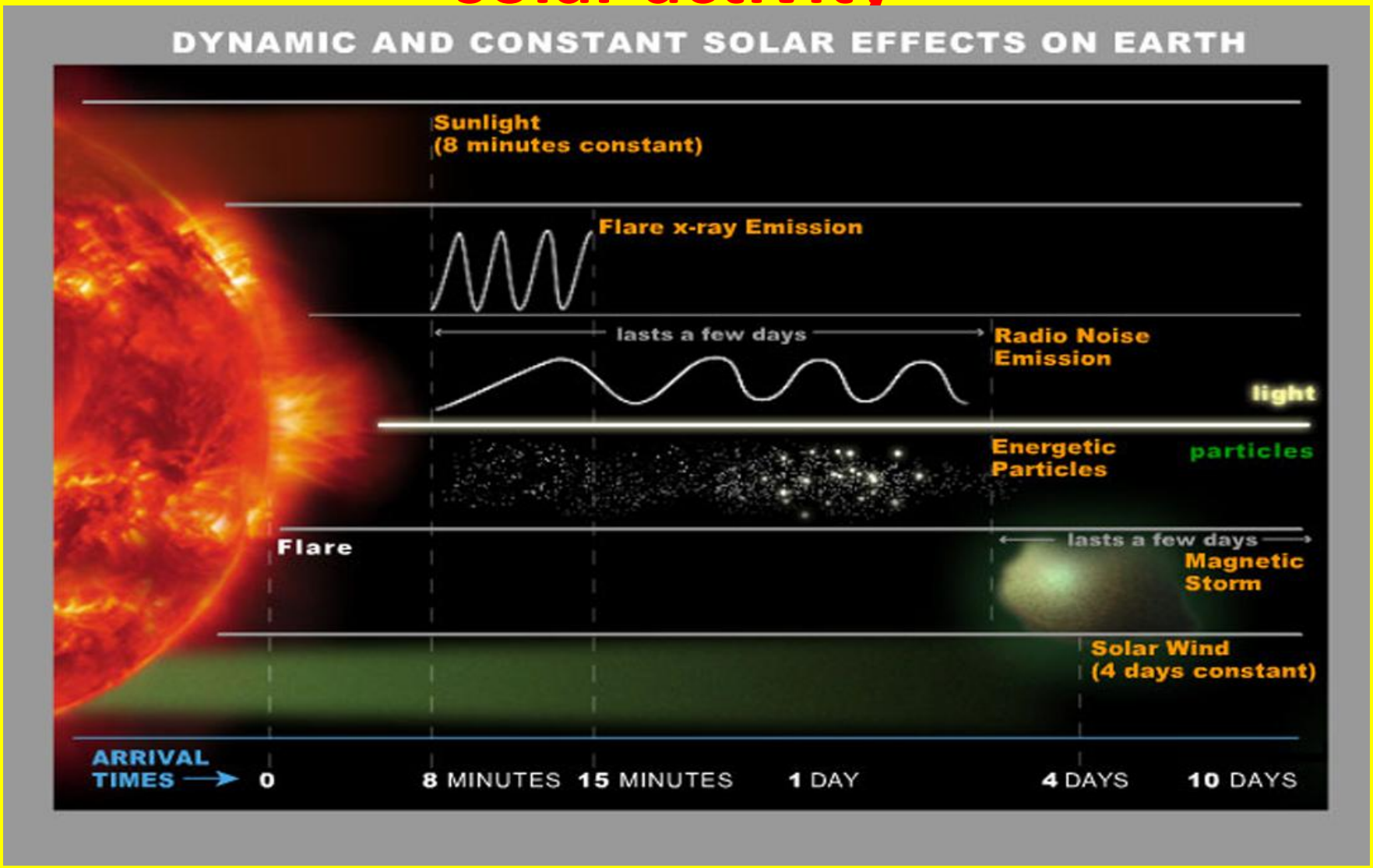

SILSO data

http://www.sidc.be/silso/ssngraphics

UKR.NET: Всі новини України... | Workshop Solar influences on... | Отправлено | Sunspot Number graphics ...

Sunspot Index and Long-term Solar Observations

Menu

- Home
- Data
- Products
  - Graphics
  - Cycle forecasts
  - Sunspot Bulletin
  - Subscribe
- Analyses
- FAQ & News
- Observers
- Contact
- Legal notices

Sunspot Number

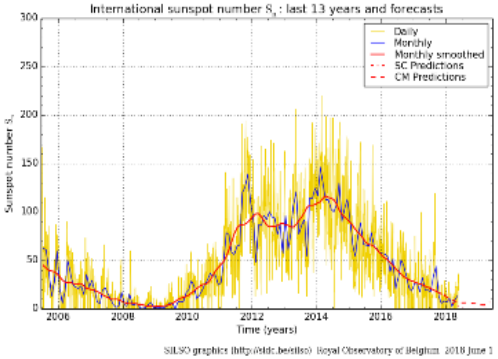

Daily, monthly and 13-month smoothed sunspot numbers for the past 13 years, and 12-month ahead predictions.

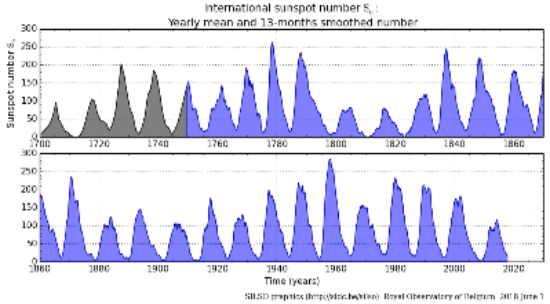

Yearly mean and 13-month smoothed monthly sunspot number since 1700.

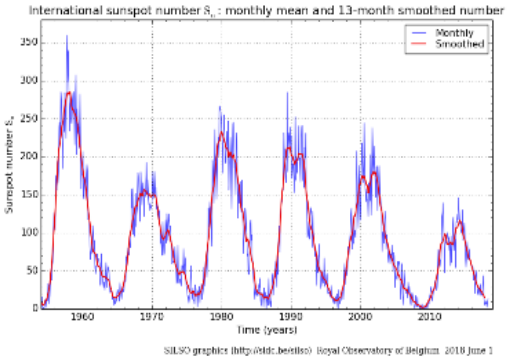

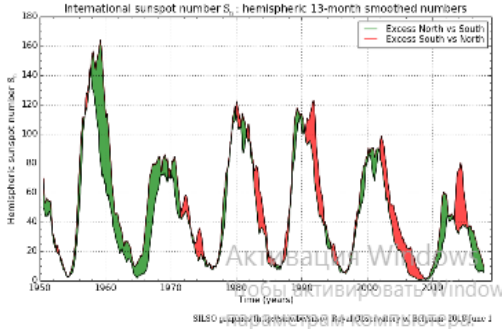

North and South hemispheric sunspot numbers (13-

Ссылки | ENG | 21:41 03.06.2018

SWPC data

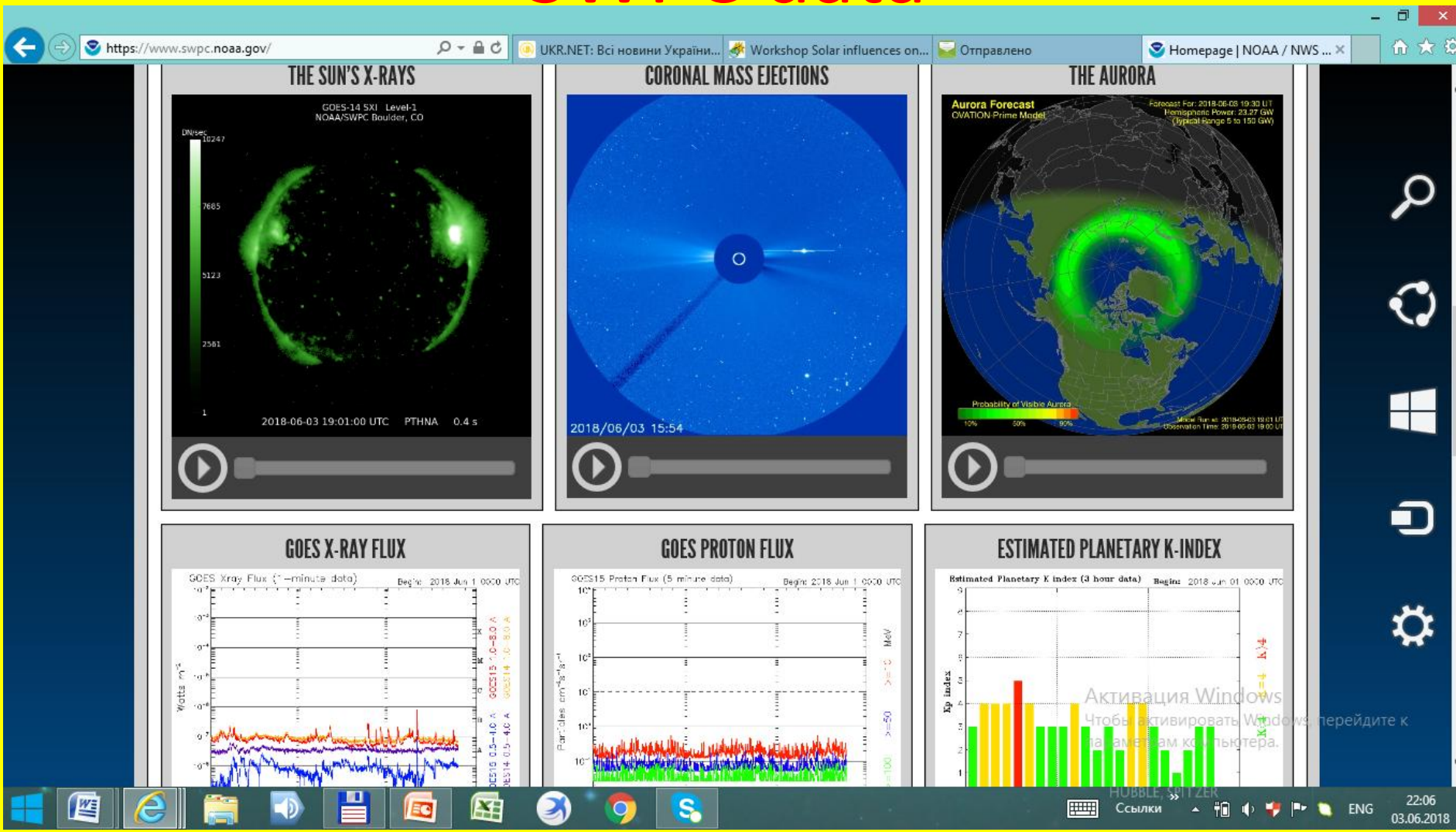
https://www.swpc.noaa.gov/
UKR.NET: Всі новини України...
Workshop Solar influences on...
Отправлено
Homepage | NOAA / NWS ...
THE SUN'S X-RAYS
GOES-14 SXI Level-1
NOAA/SWPC Boulder, CO
2018-06-03 19:01:00 UTC PTHNA 0.4 s
CORONAL MASS EJECTIONS
2018/06/03 15:54
THE AURORA
Aurora Forecast
OVATION Prime Model
GOES X-RAY FLUX
GOES PROTON FLUX
ESTIMATED PLANETARY K-INDEX
Estimated Planetary K index (3 hour data)
Kp index
Активация Windows
Ссылки
ENG
22:06
03.06.2018

What's the problem?

- **The basis of presentation about the Sun cycle activity the monthly mean values of major indexes and their fluctuation values.**

- **On their basis is formed by an idea of continuity of monotony and solar cycle.**
- **These views are based on statistical data, and does not reflect the physical properties of the manifestations of the solar cycle.**
-

Variants of daily index of solar activity and solar-terrestrial relations

- W- Wolf Numbers (calculation)
- SpN – SpS the summary area of groups of spots (Total, Northern and Southern hemispheres)
- F 10.7 cm – flux of radioemission (observation
- Parameters of solar wind (velocity, pressure) – observations .
- Index of geomagnetic activity – observations
- And many others!

“Correlation” of Solar indexes:W, F10, FI, SI

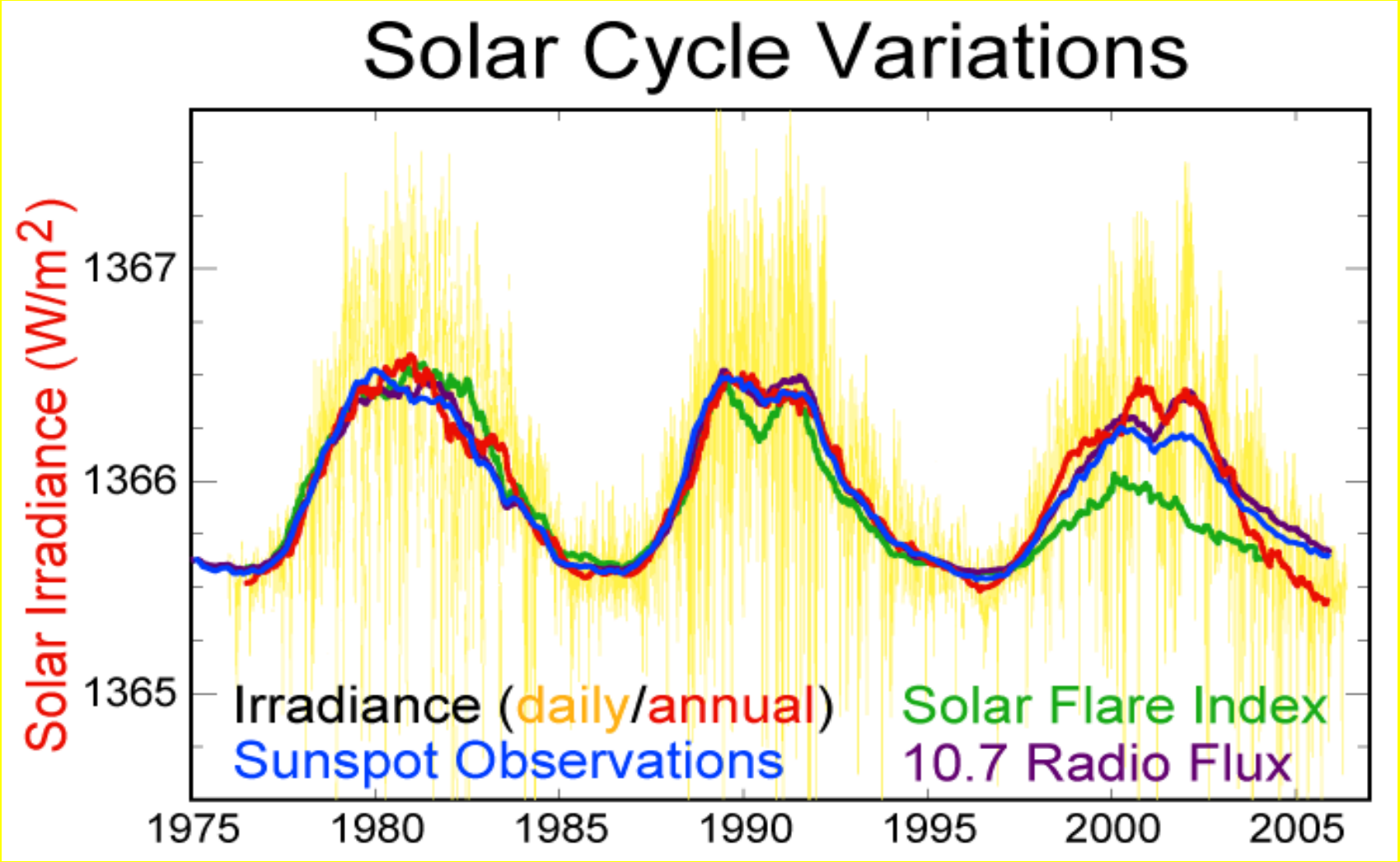

W

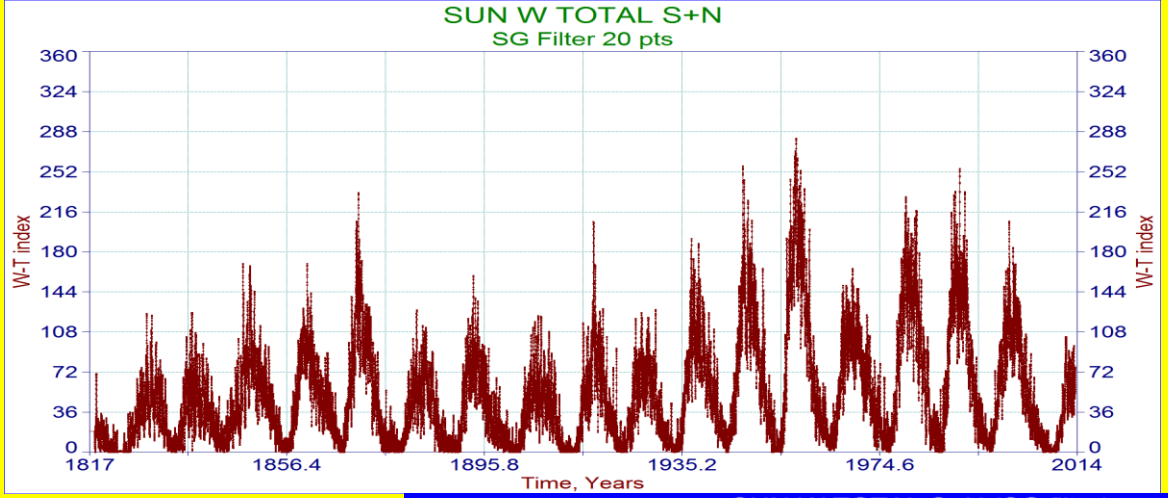

Periods

6 years – 20 days

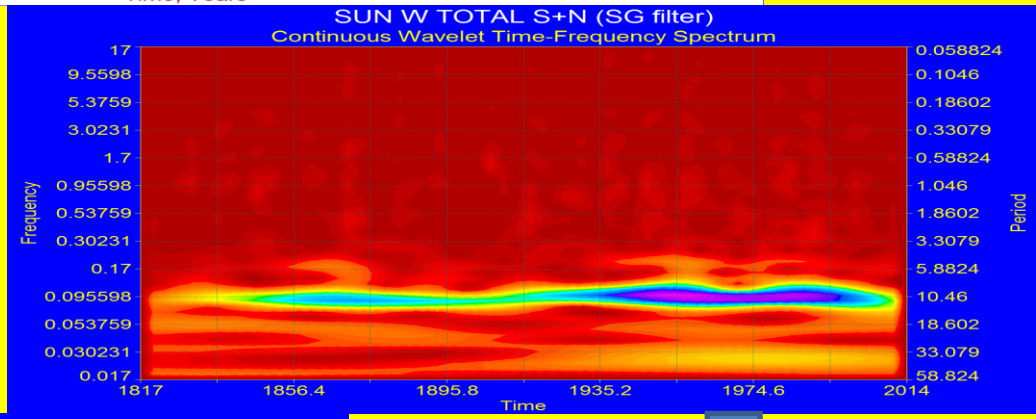

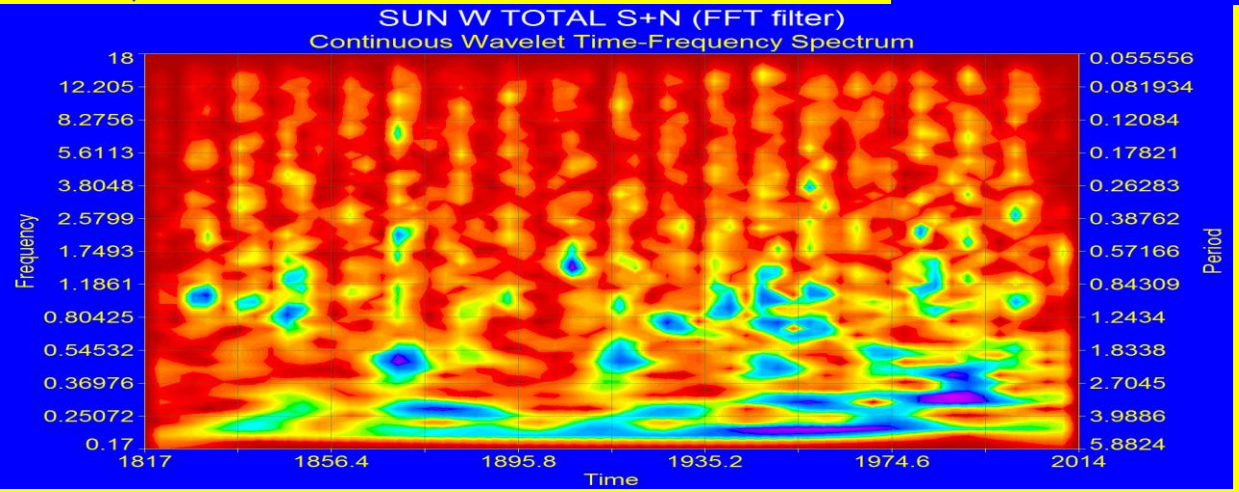

“11 -th” cycle

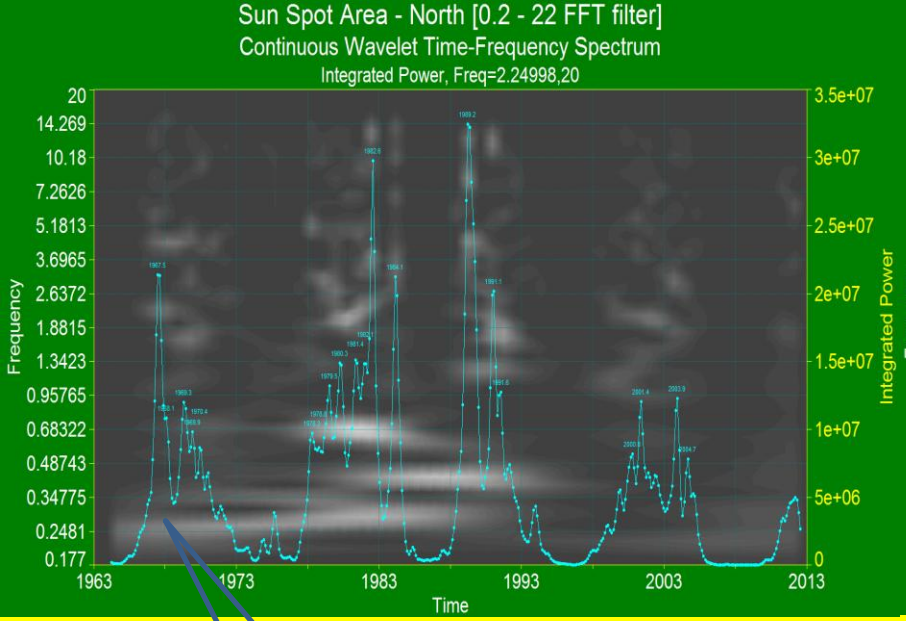

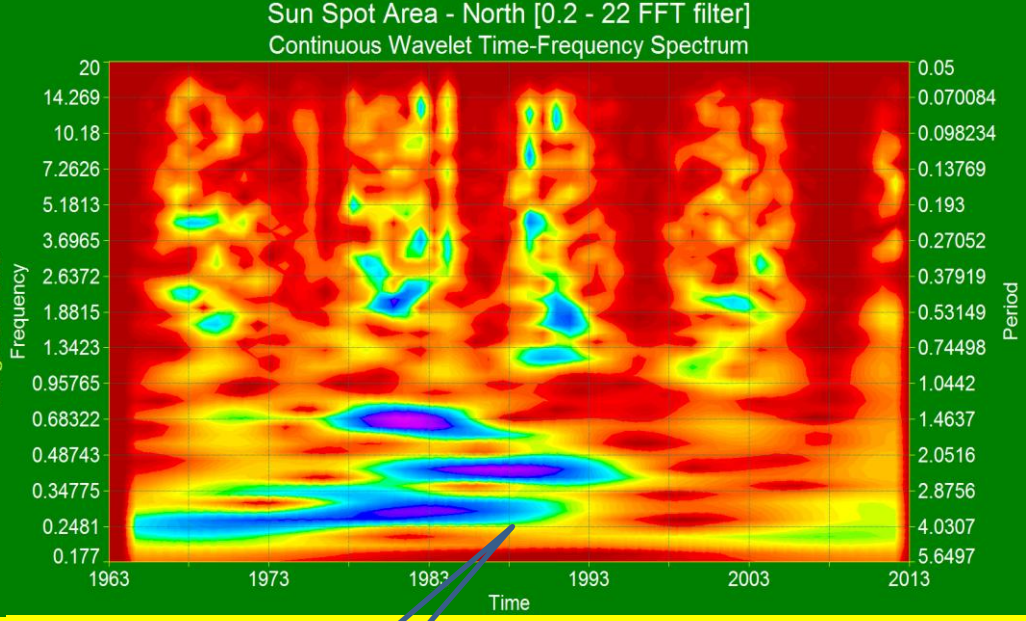

SpN

SpS

SpN

SpS

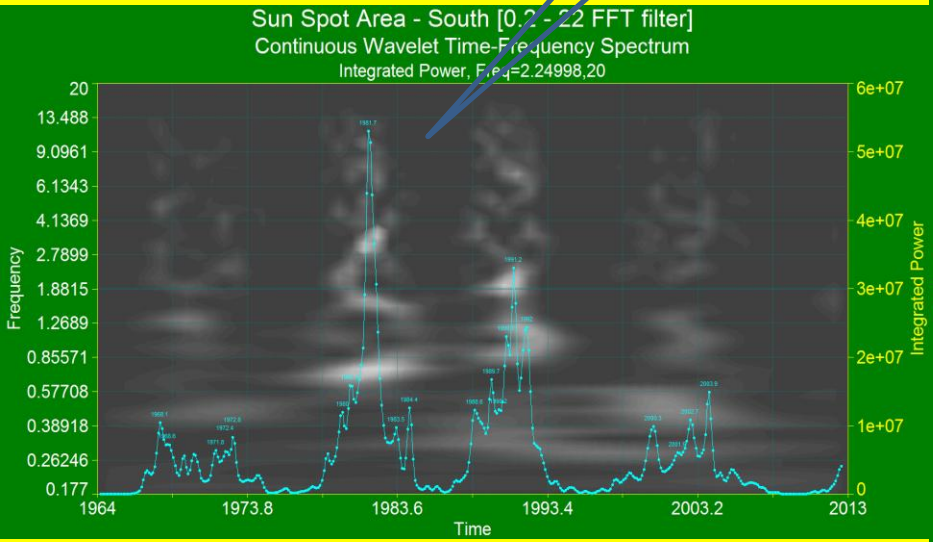

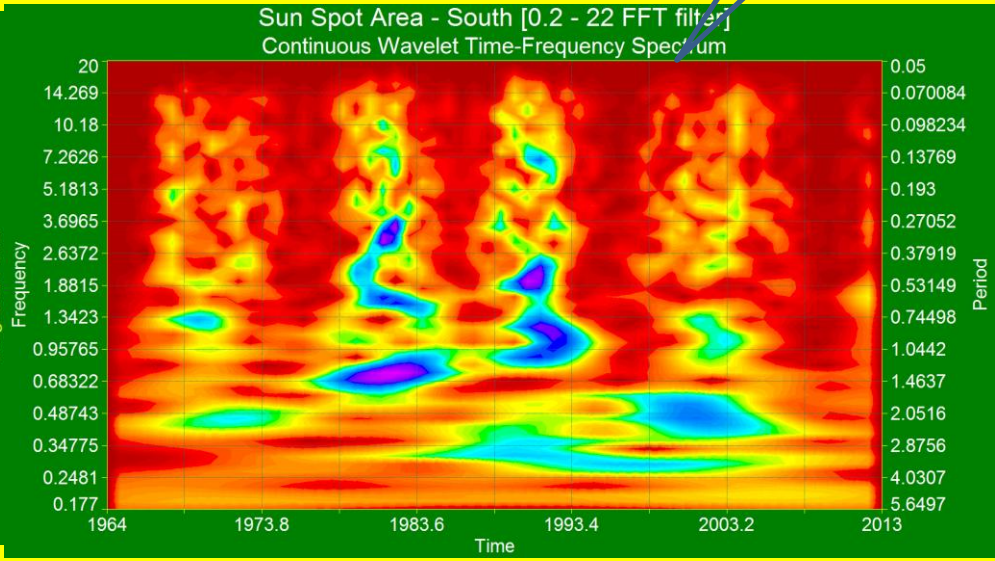

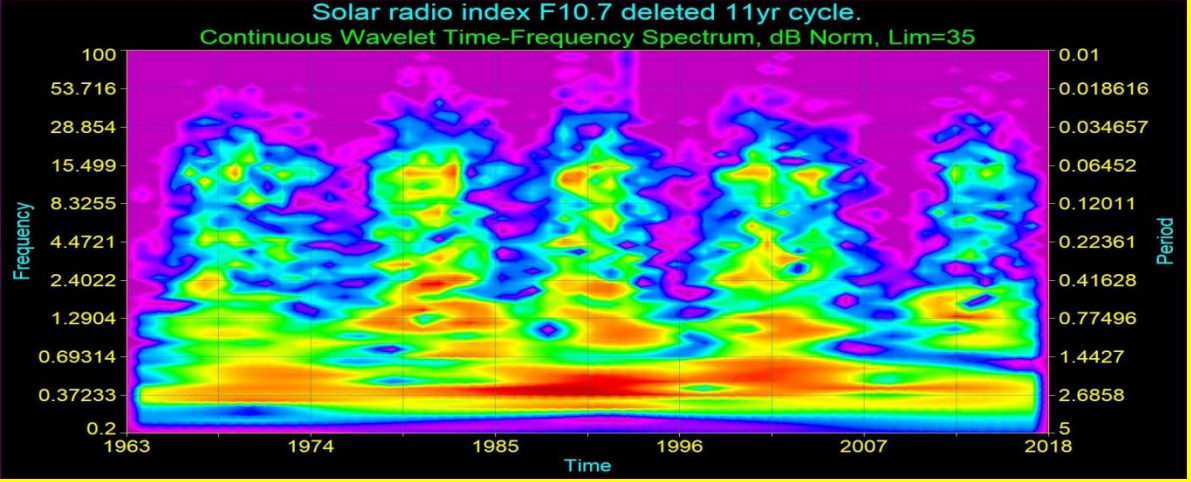

20-24 cycles (F 10.7)

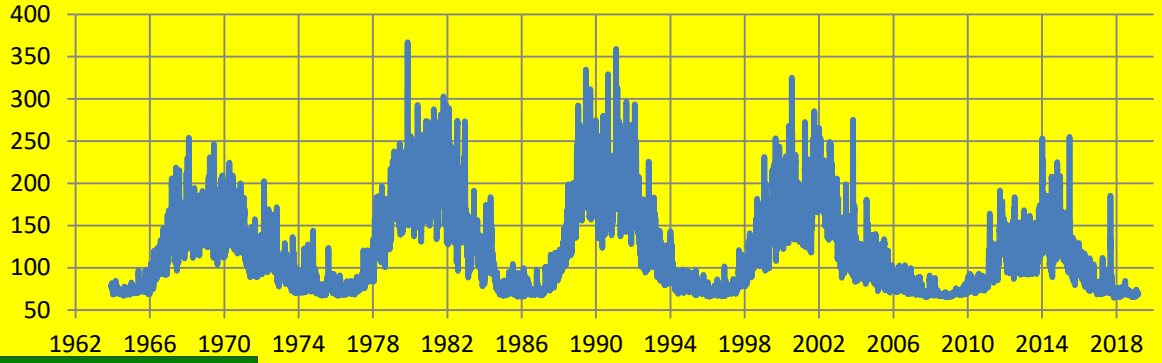

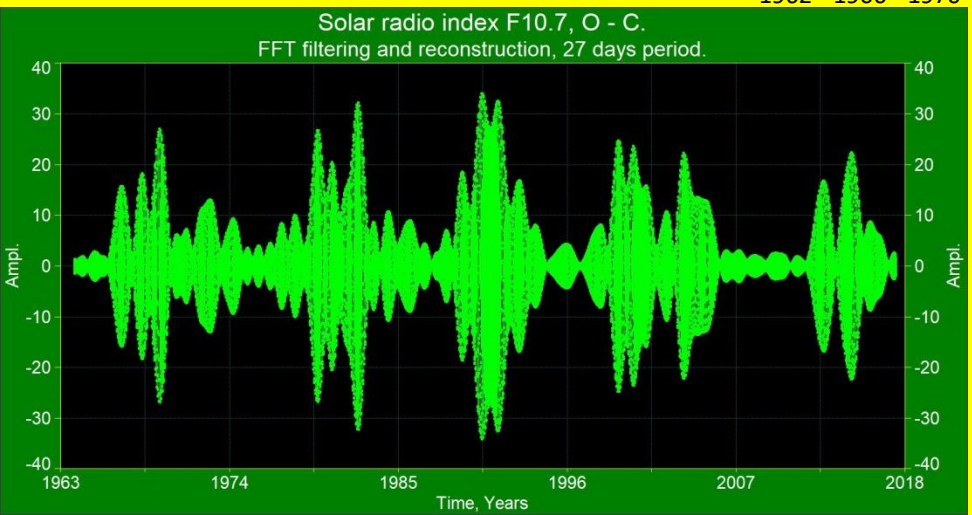

Observation data

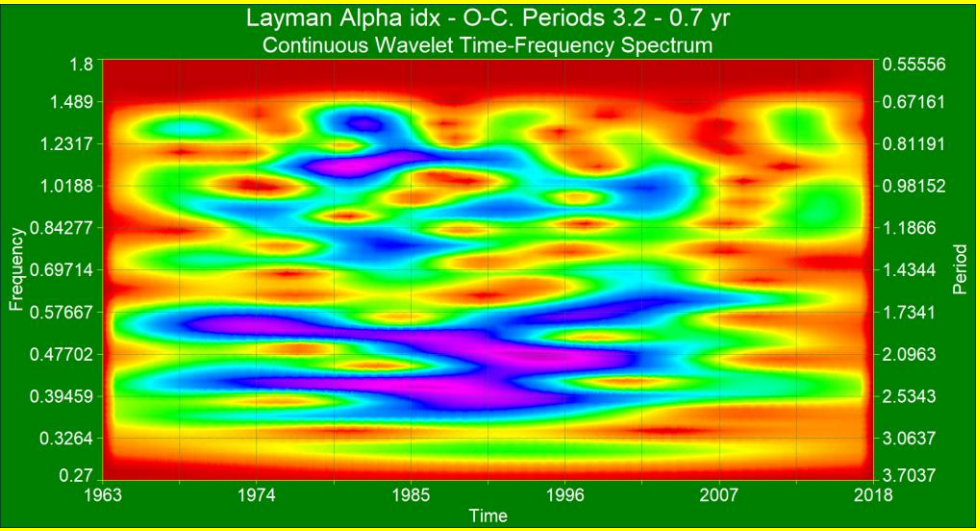

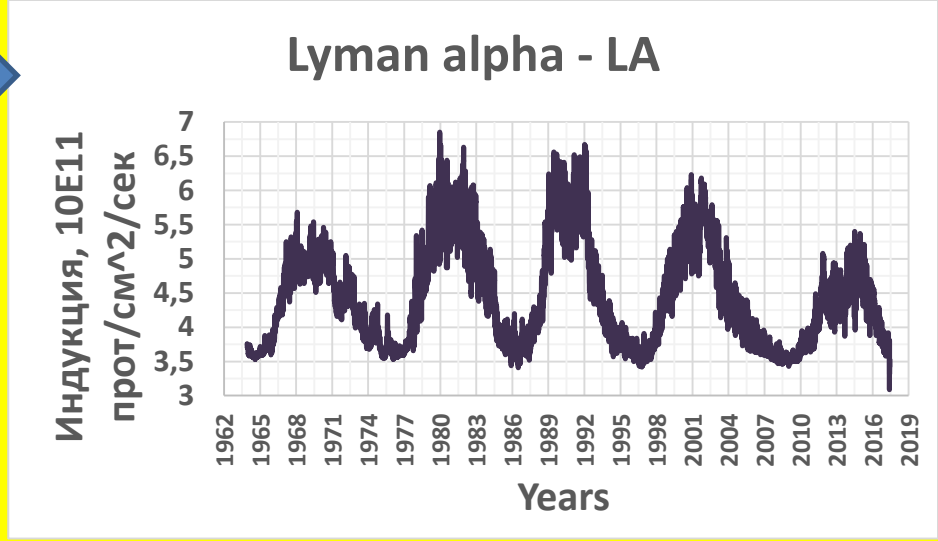

27d

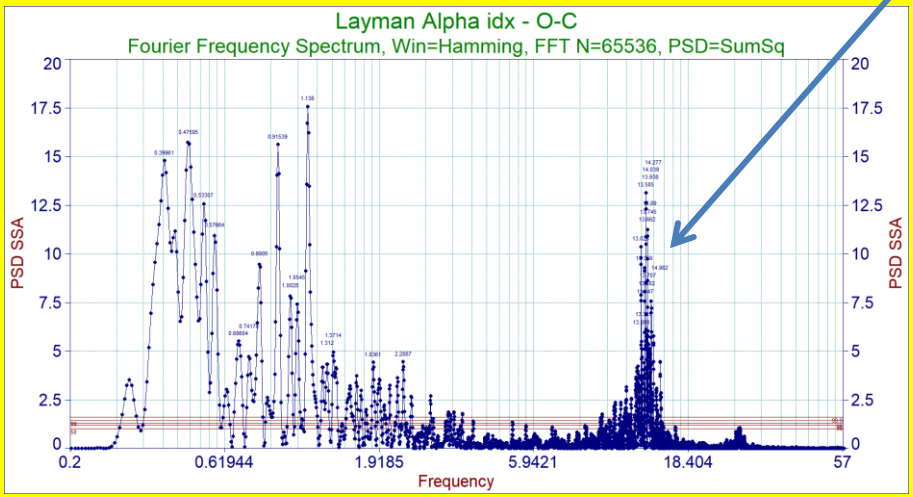

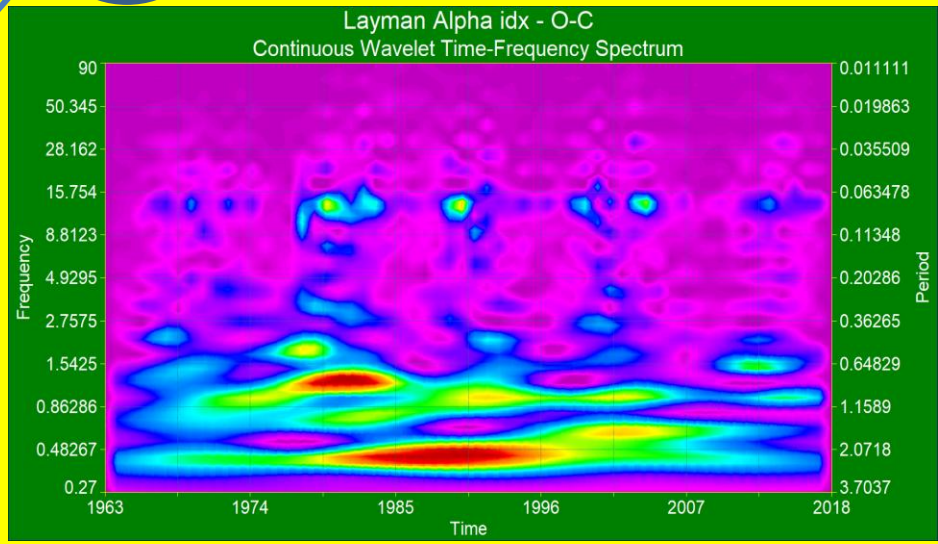

«Spotless» cycles

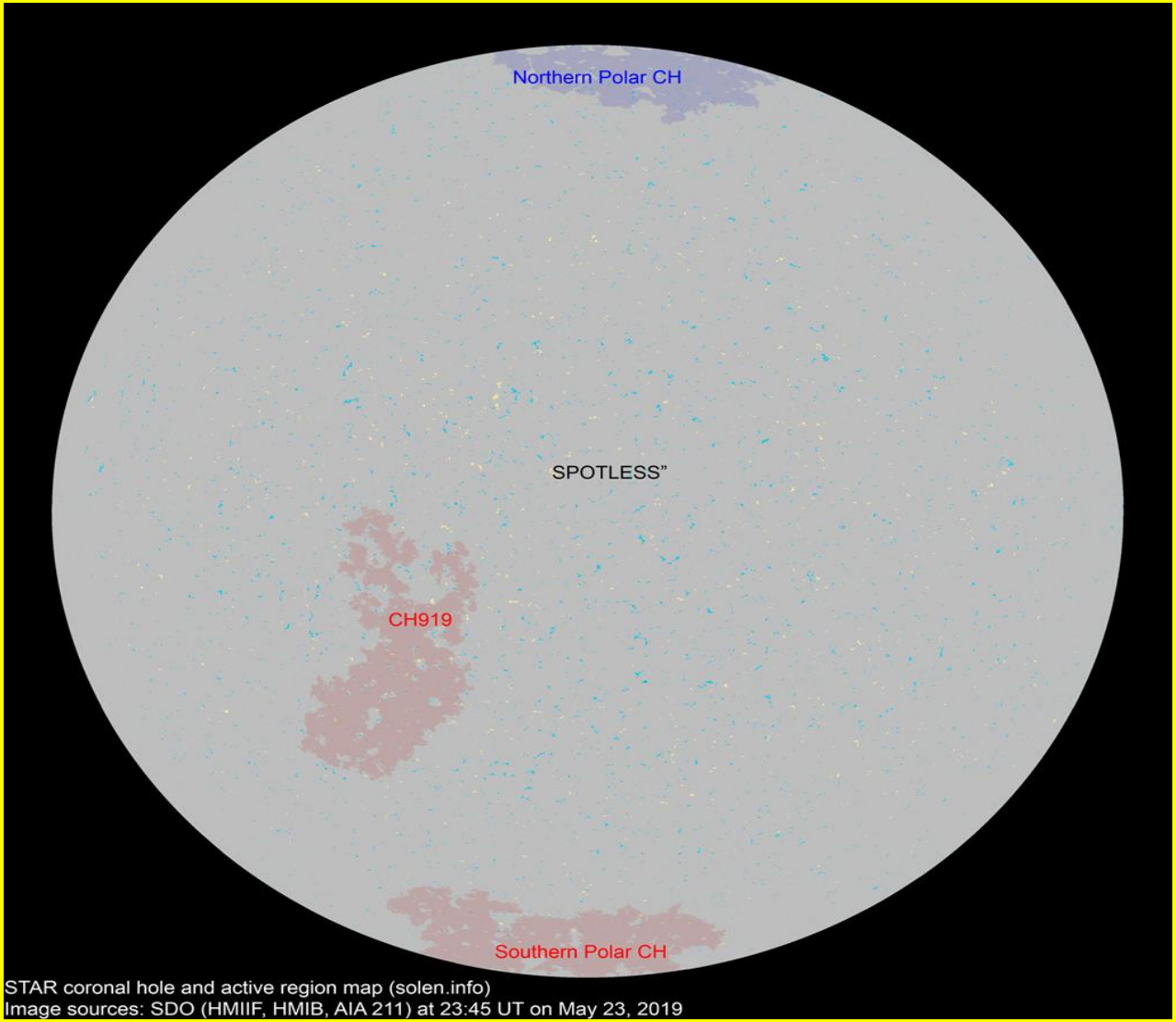

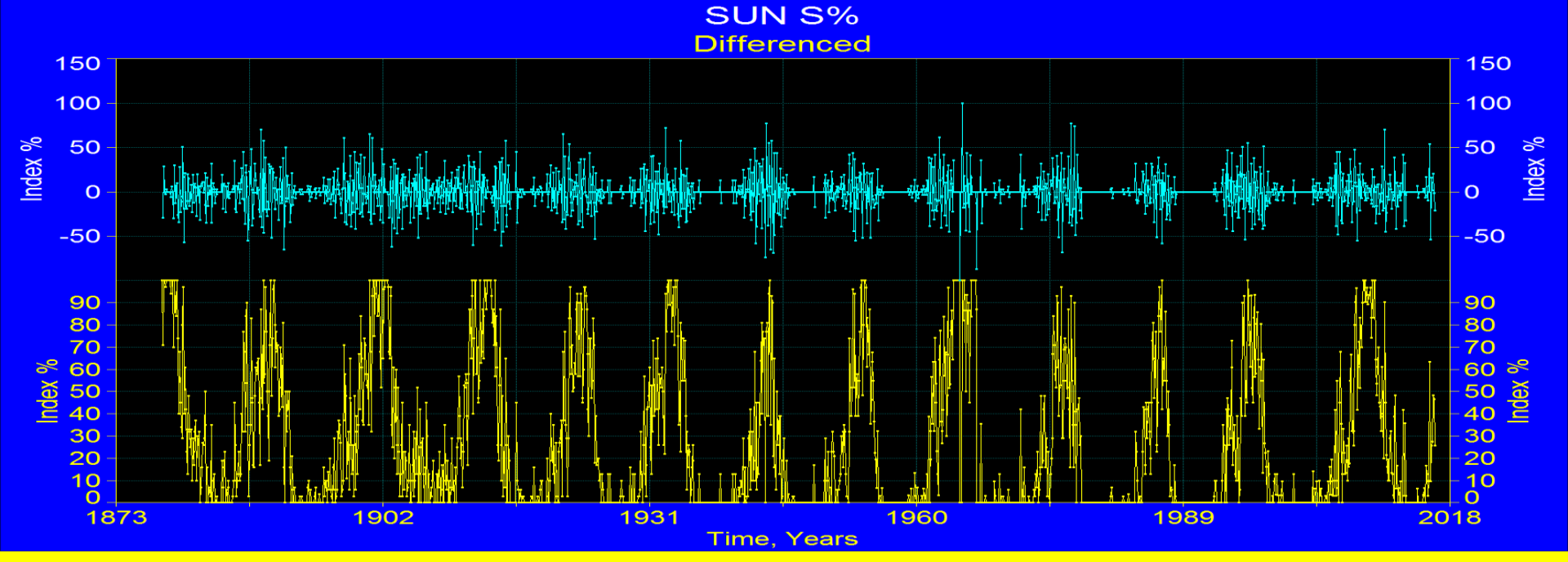
SUN S%
Differenced
150
100
50
0
-50
Index %
90
80
70
60
50
40
30
20
10
0
1873
1902
1931
1960
1989
2018
Time, Years

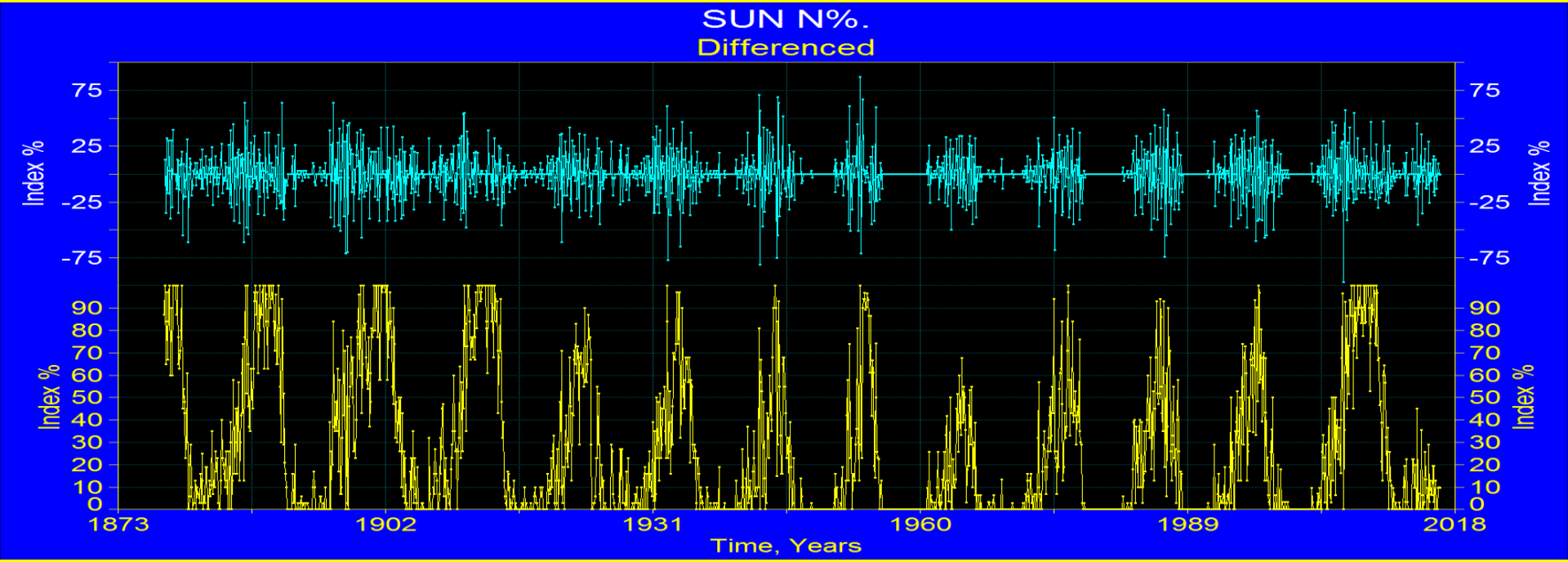
SUN N%.
Differenced
75
25
-25
-75
Index %
90
80
70
60
50
40
30
20
10
0
1873
1902
1931
1960
1989
2018
Time, Years

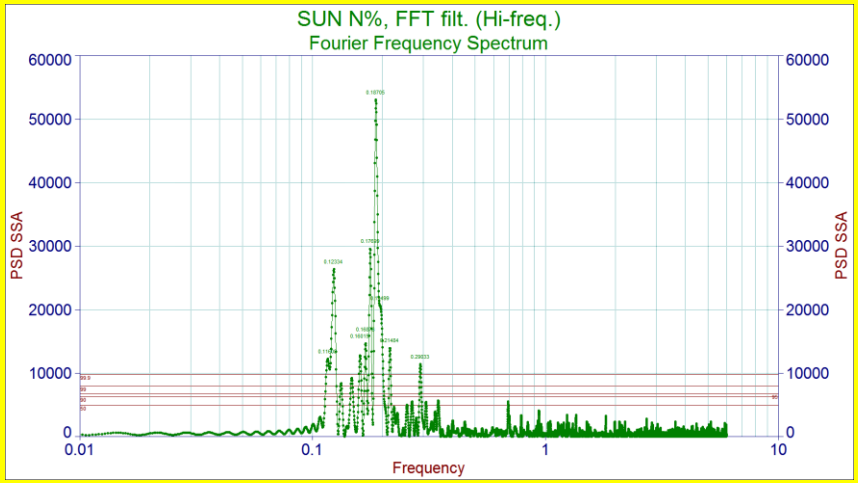
SUN N%, FFT filt. (Hi-freq.)
Fourier Frequency Spectrum
PSD SSA
Frequency
60000
50000
40000
30000
20000
10000
0
0.01
0.1
1
10

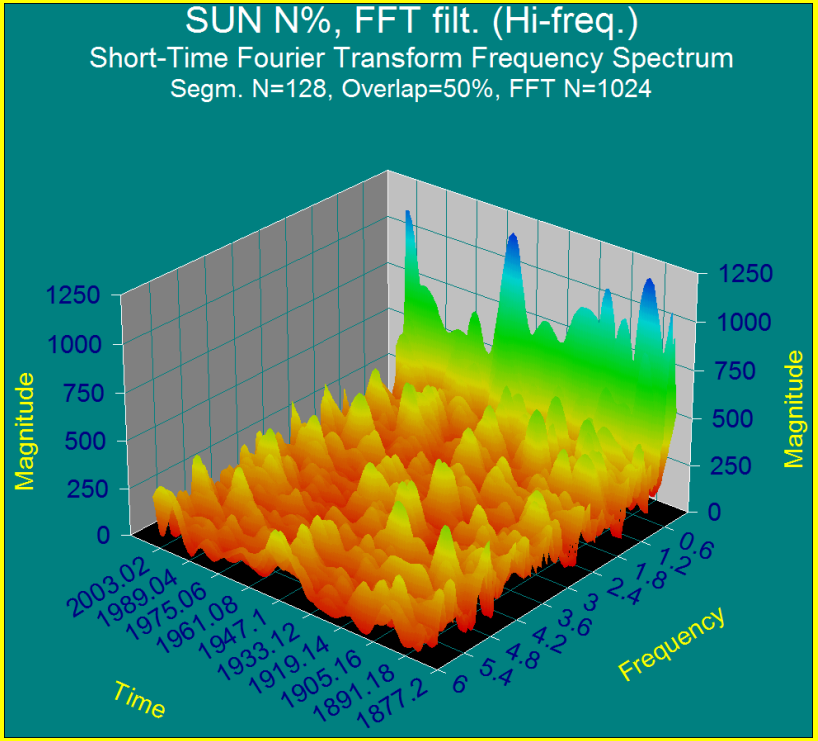
SUN N%, FFT filt. (Hi-freq.)
Short-Time Fourier Transform Frequency Spectrum
Segm. N=128, Overlap=50%, FFT N=1024
Magnitude
Time
Frequency
1250
1000
750
500
250
0
2003.02
1989.04
1975.06
1961.08
1947.1
1933.12
1919.14
1905.16
1891.18
1877.2

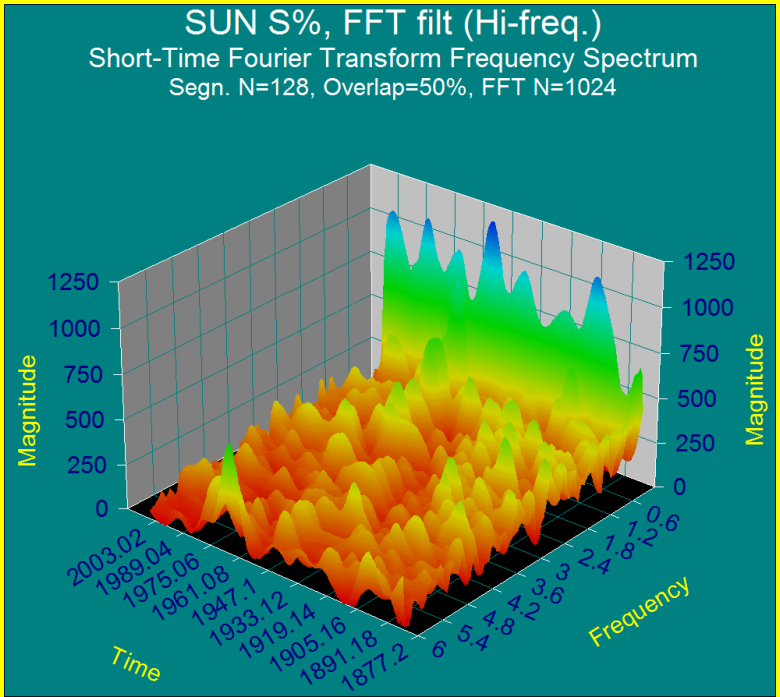
SUN S%, FFT filt (Hi-freq.)
Short-Time Fourier Transform Frequency Spectrum
Segn. N=128, Overlap=50%, FFT N=1024
Magnitude
Time
Frequency
1250
1000
750
500
250
0
2003.02
1989.04
1975.06
1961.08
1947.1
1933.12
1919.14
1905.16
1891.18
1877.2

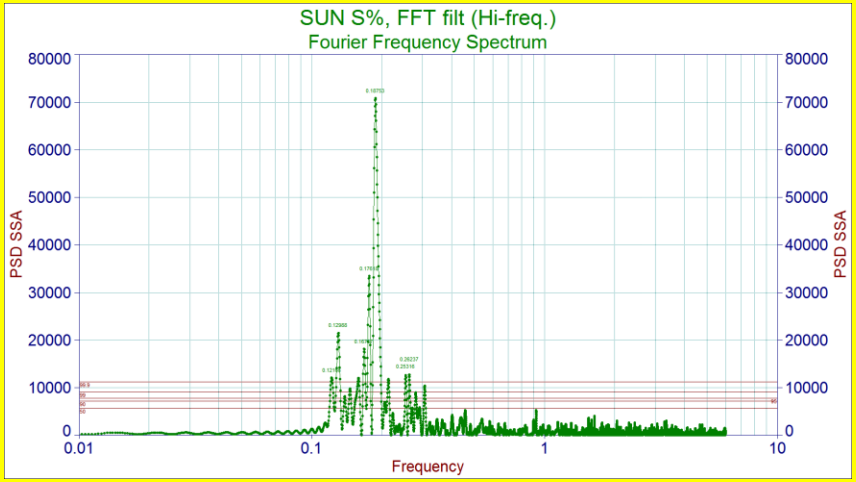
SUN S%, FFT filt (Hi-freq.)
Fourier Frequency Spectrum
PSD SSA
Frequency
80000
70000
60000
50000
40000
30000
20000
10000
0
0.01
0.1
1
10

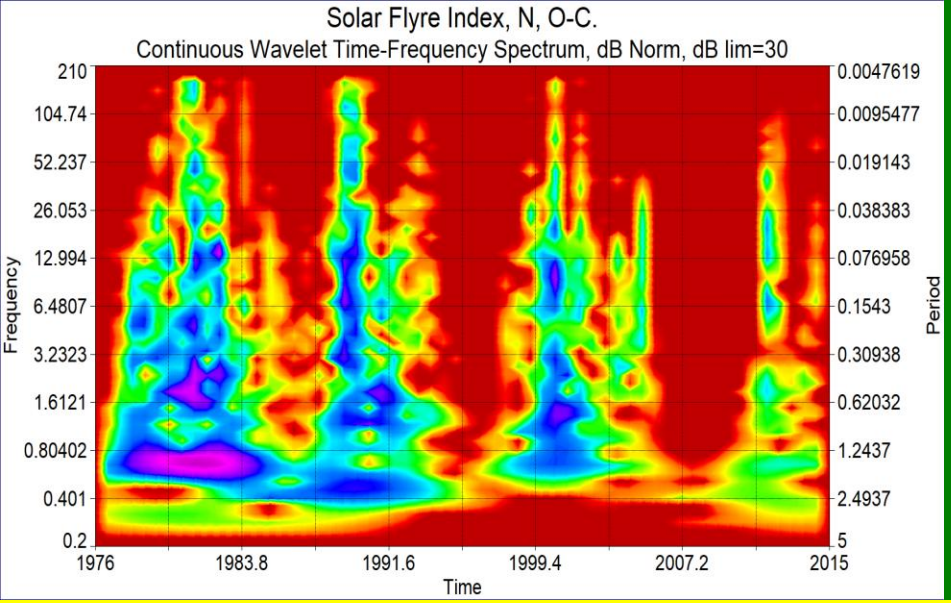

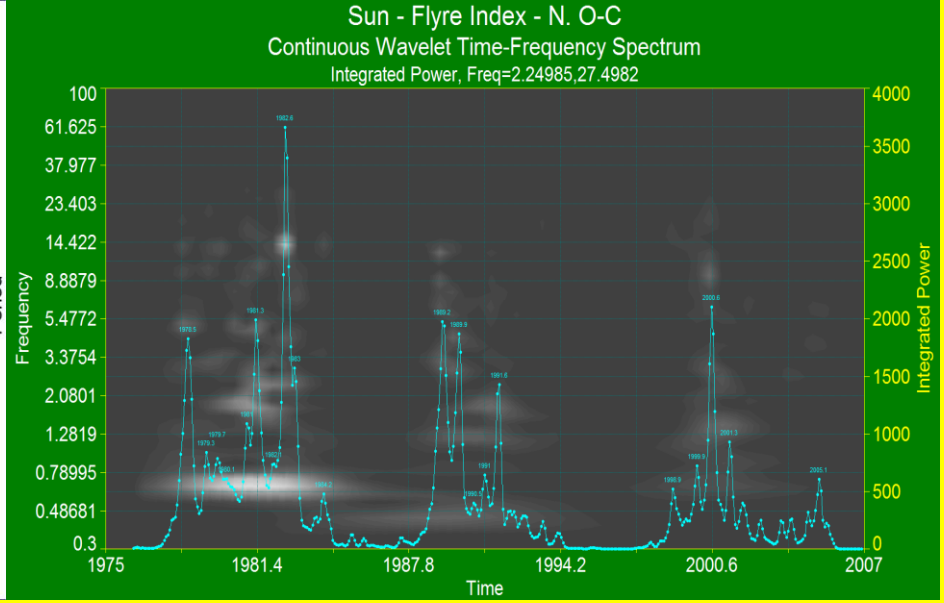

Flare Index - Spectrum and Phase Activity

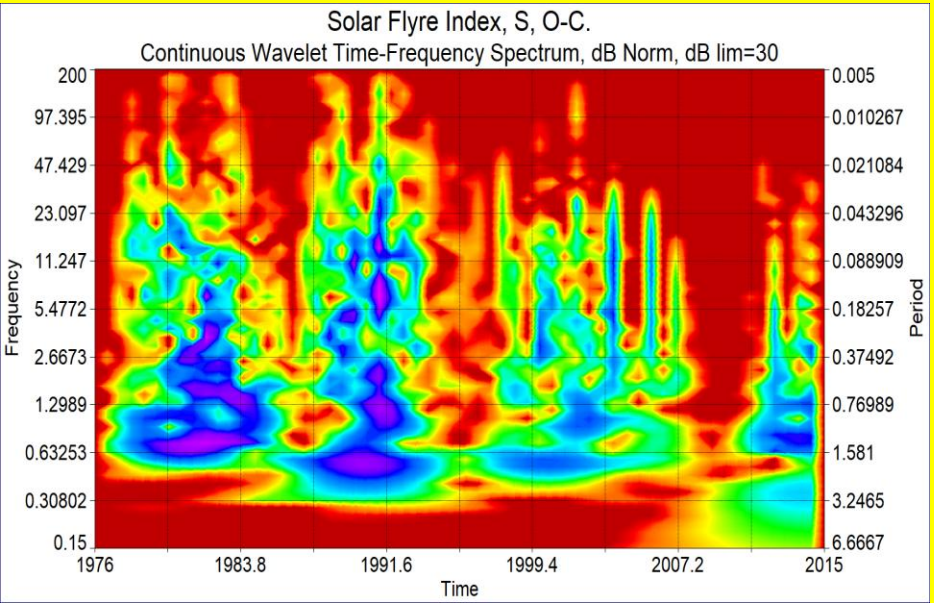

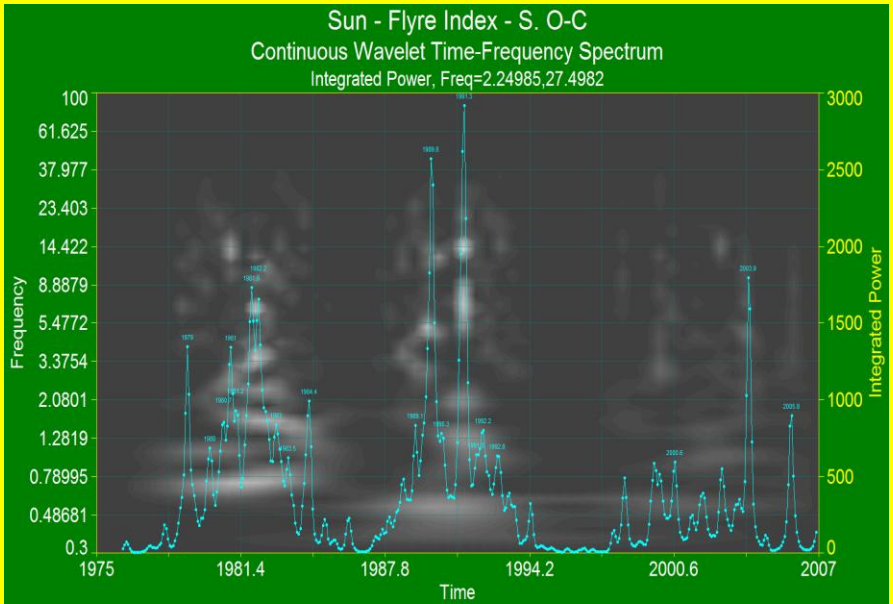

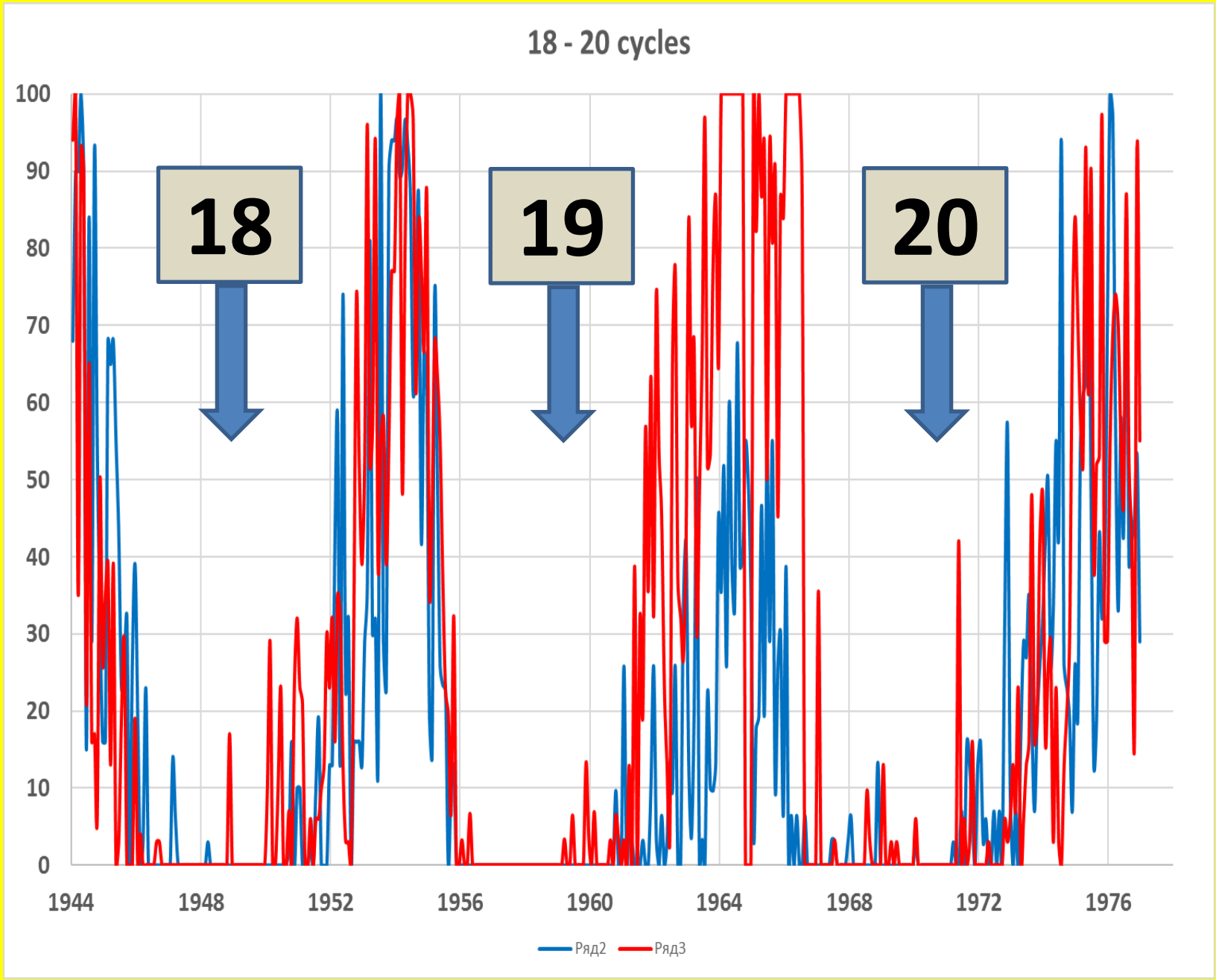
18 - 20 cycles
18
19
20
100
90
80
70
60
50
40
30
20
10
0
1944
1948
1952
1956
1960
1964
1968
1972
1976
Ряд2
Ряд3

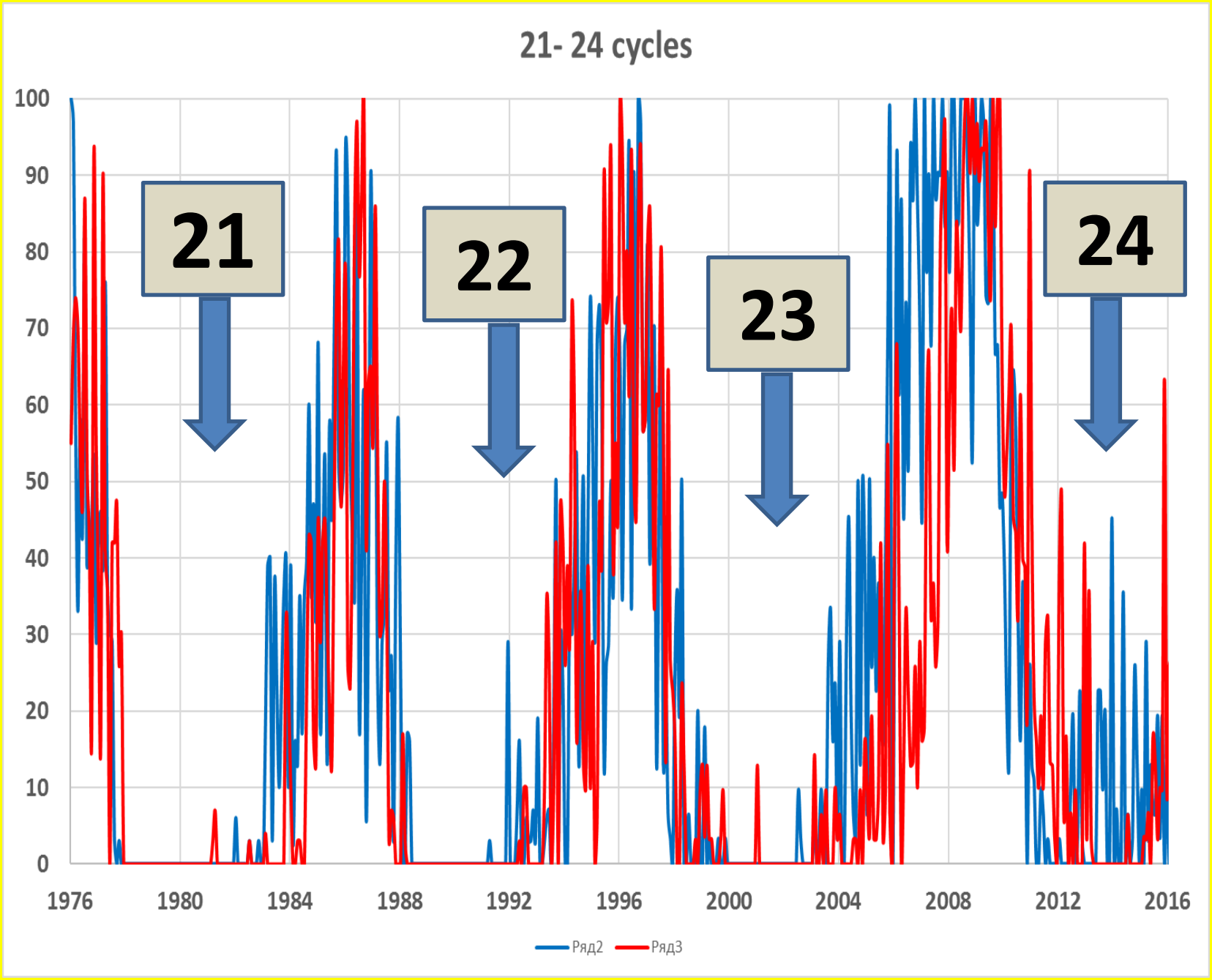
21- 24 cycles
100
90
80
70
60
50
40
30
20
10
0
1976
1980
1984
1988
1992
1996
2000
2004
2008
2012
2016
21
22
23
24
Ряд2
Ряд3

N and S solar spotless cycles

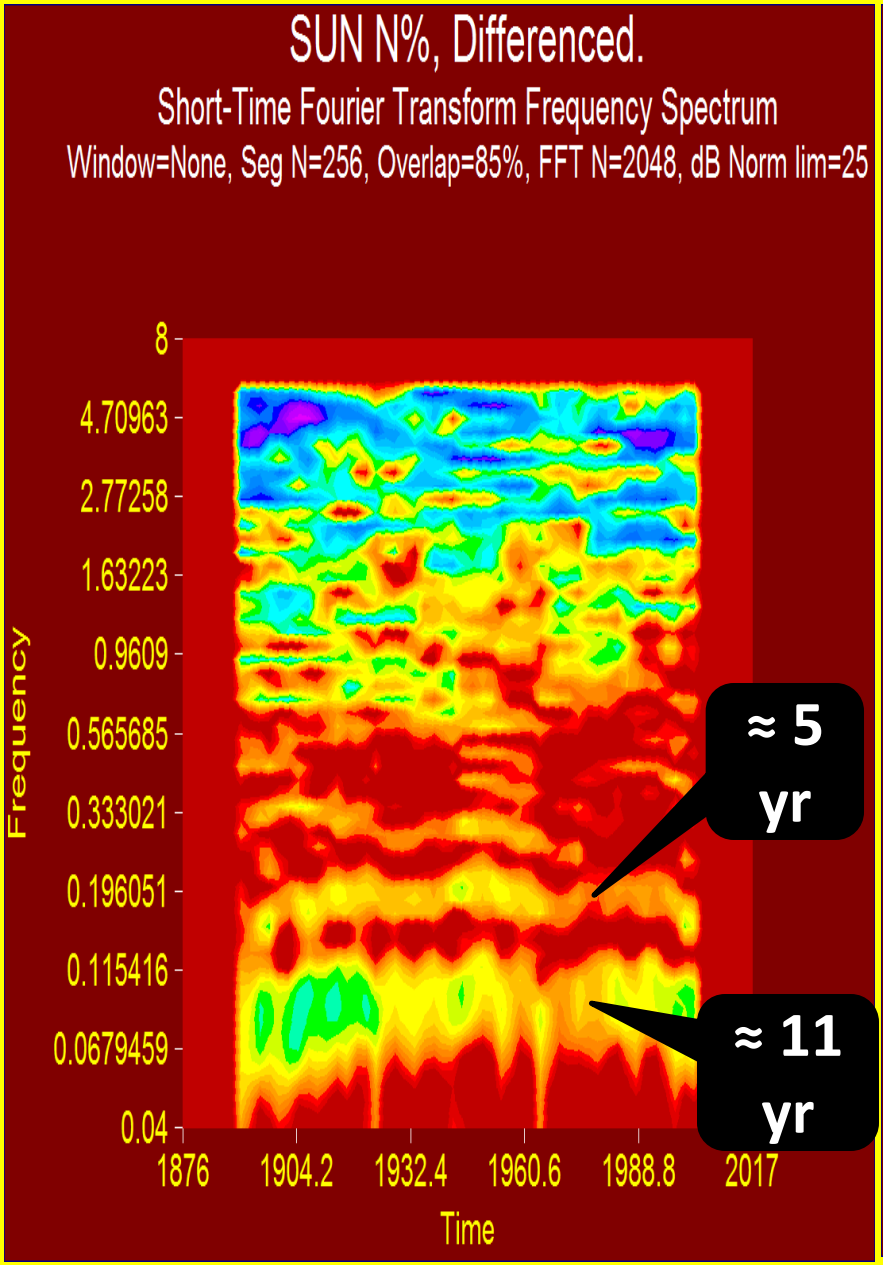

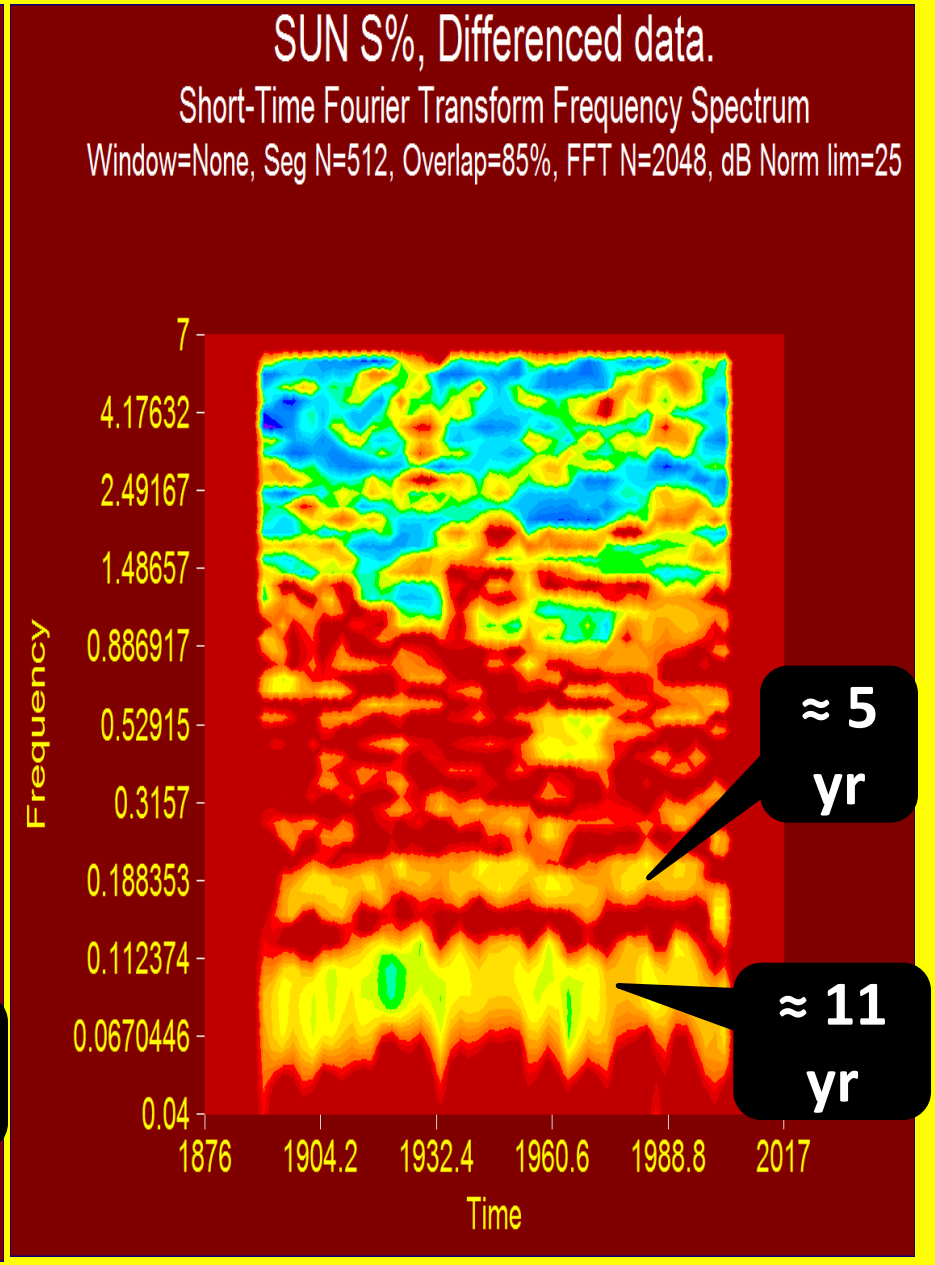

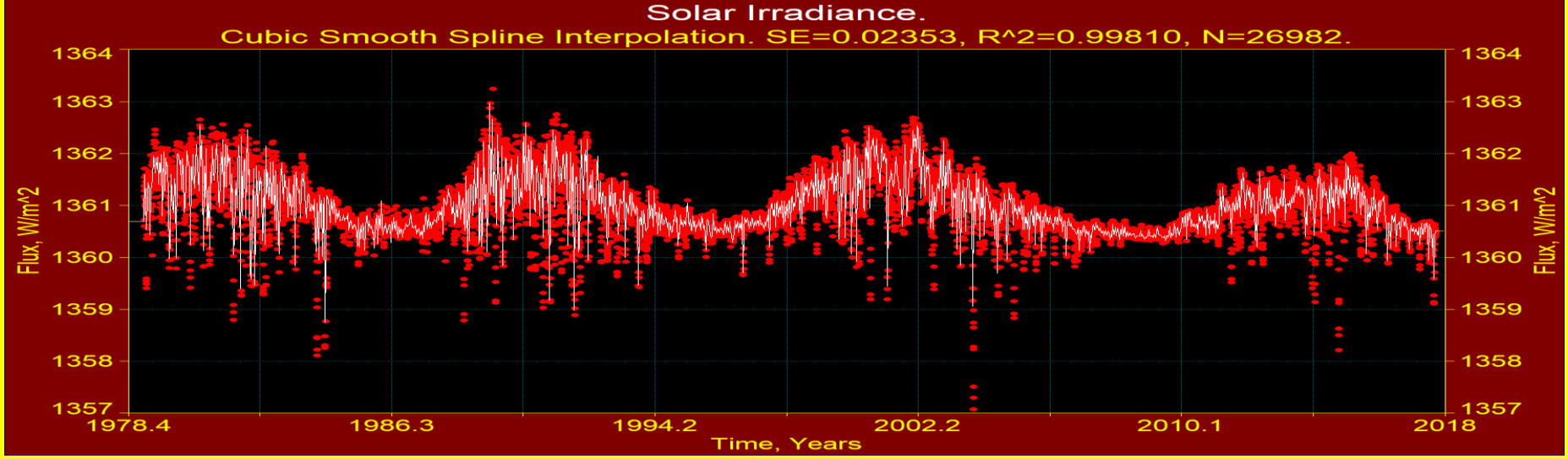
Solar Irradiance.
Cubic Smooth Spline Interpolation. SE=0.02353, R^2=0.99810, N=26982.
Flux, W/m^2
1364
1363
1362
1361
1360
1359
1358
1357
1978.4
1986.3
1994.2
2002.2
2010.1
2018
Time, Years

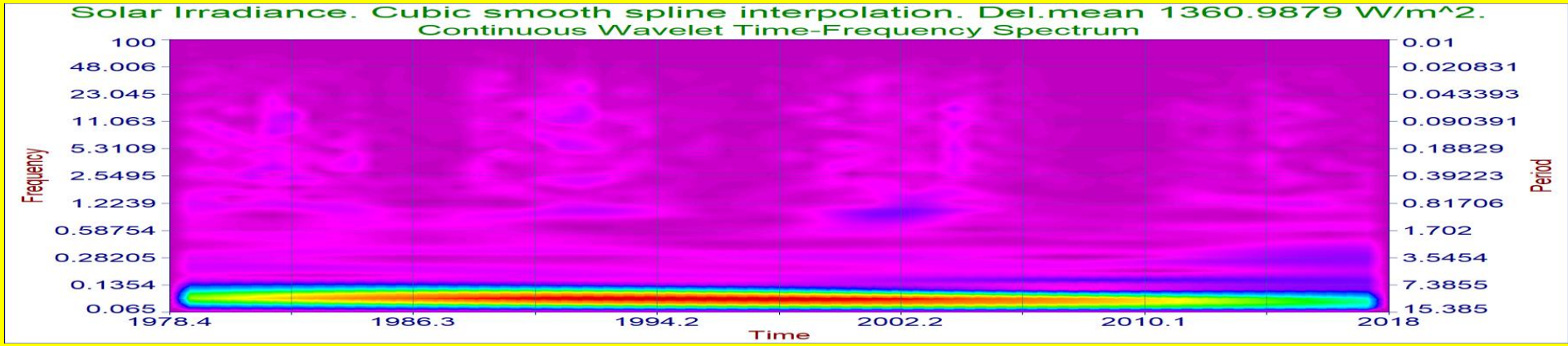
Solar Irradiance. Cubic smooth spline interpolation. Del.mean 1360.9879 W/m^2.
Continuous Wavelet Time-Frequency Spectrum
Frequency
100
48.006
23.045
11.063
5.3109
2.5495
1.2239
0.58754
0.28205
0.1354
0.065
Period
0.01
0.020831
0.043393
0.090391
0.18829
0.39223
0.81706
1.702
3.5454
7.3855
15.385
1978.4
1986.3
1994.2
2002.2
2010.1
2018
Time

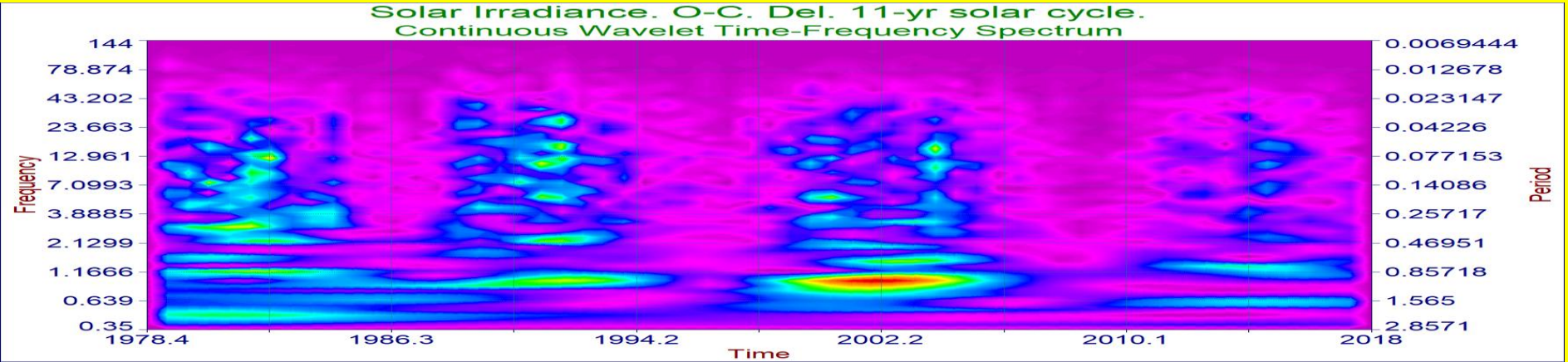
Solar Irradiance. O-C. Del. 11-yr solar cycle.
Continuous Wavelet Time-Frequency Spectrum
Frequency
144
78.874
43.202
23.663
12.961
7.0993
3.8885
2.1299
1.1666
0.639
0.35
Period
0.0069444
0.012678
0.023147
0.04226
0.077153
0.14086
0.25717
0.46951
0.85718
1.565
2.8571
1978.4
1986.3
1994.2
2002.2
2010.1
2018
Time

Sun spots component

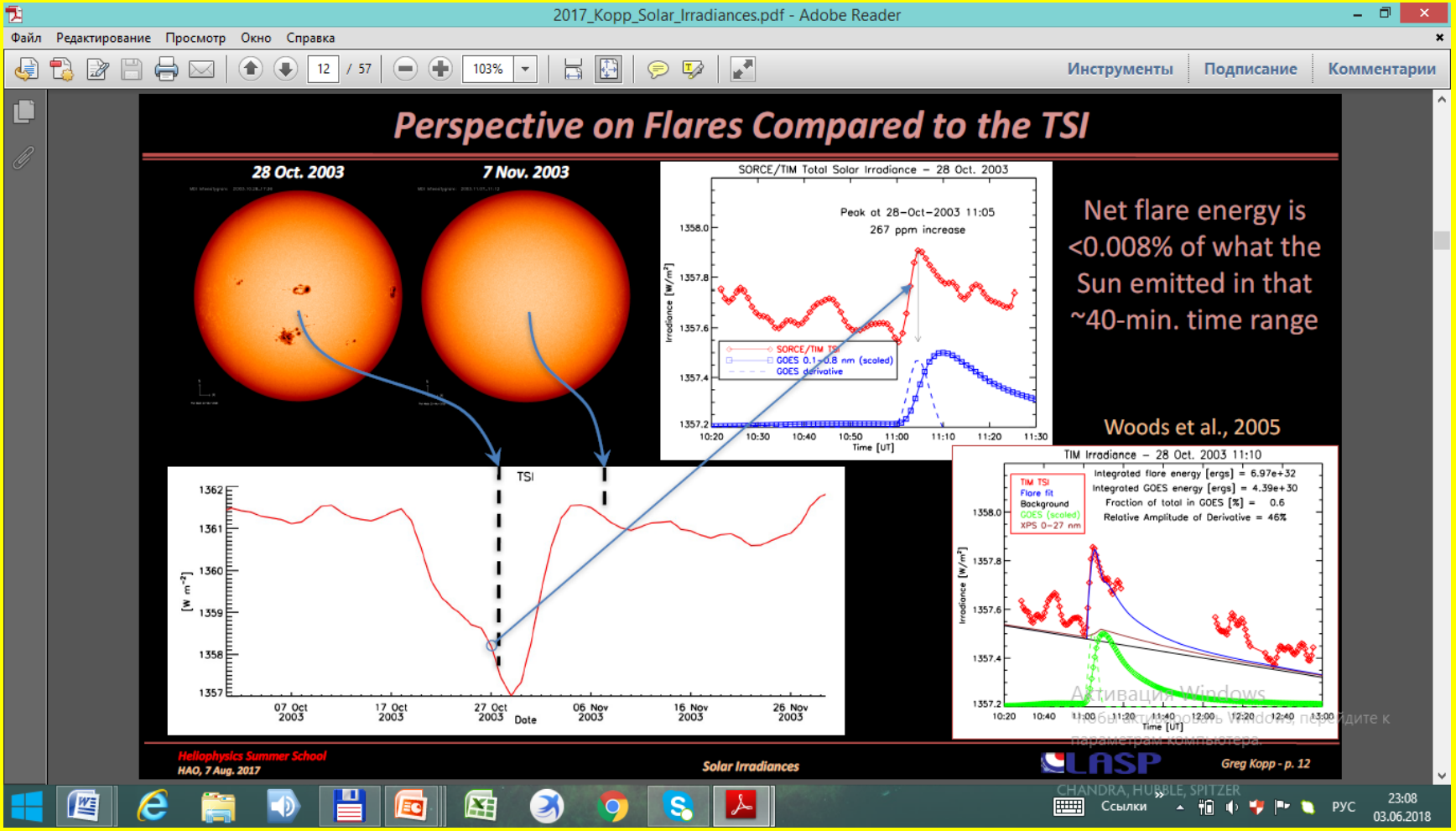

Effect directionally Solar Constant

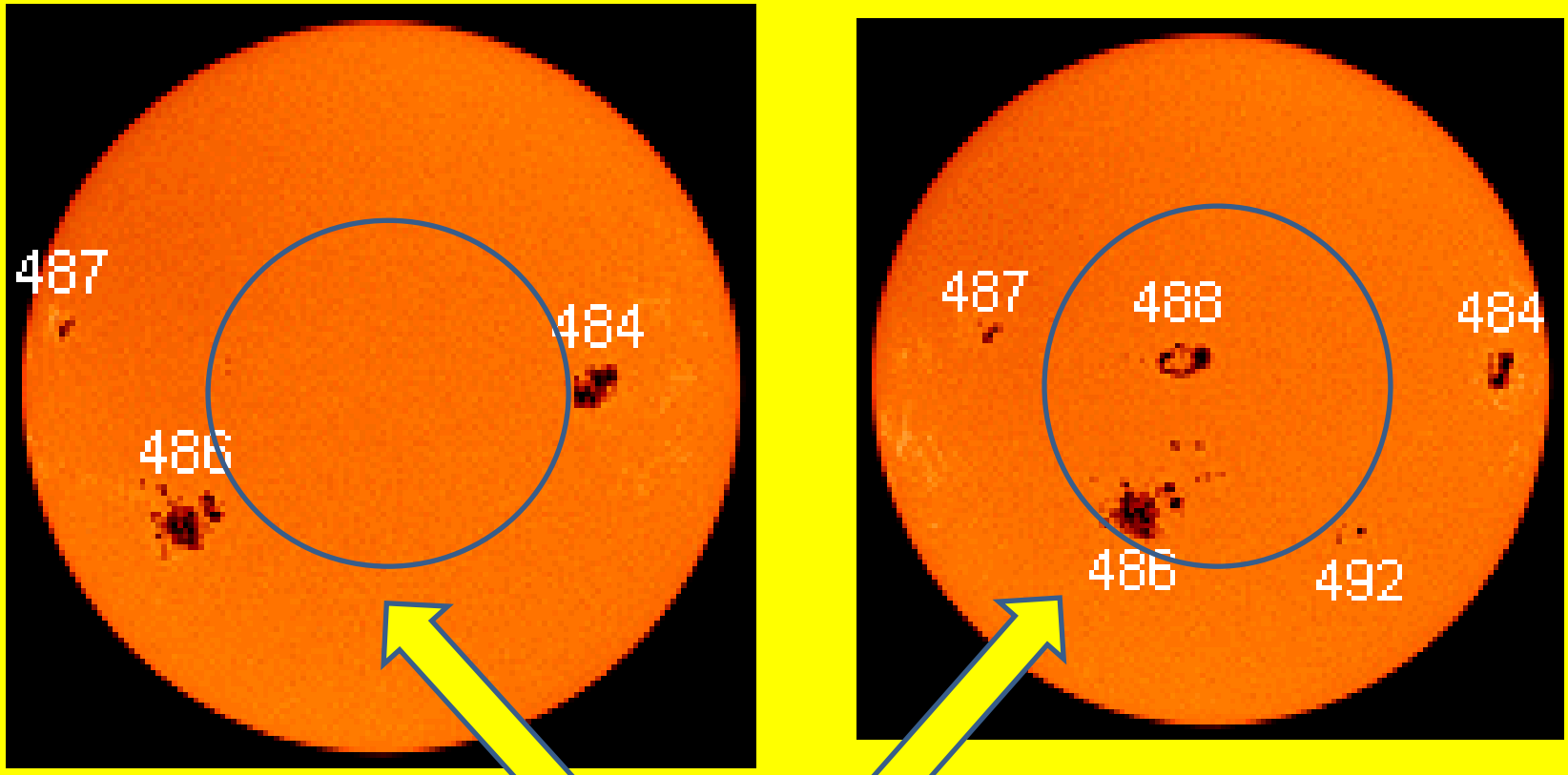

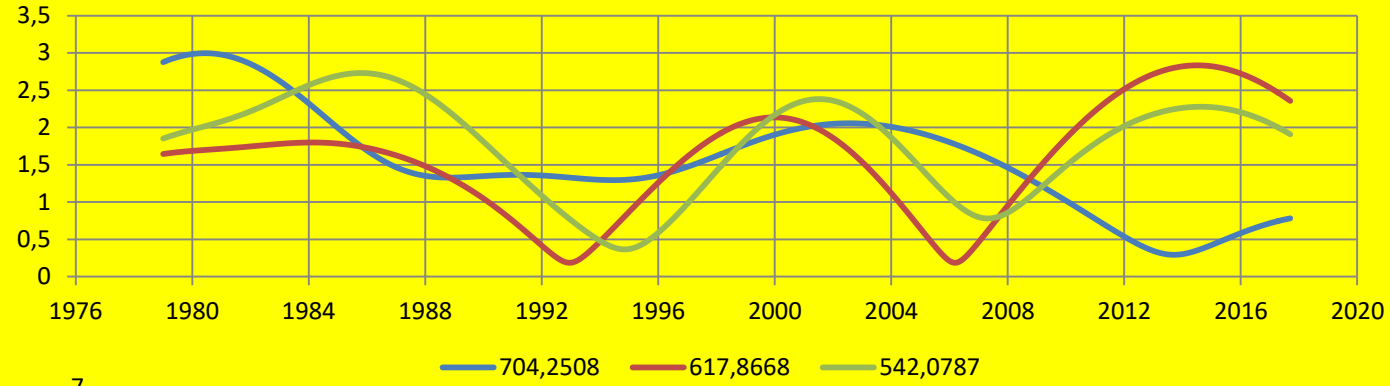
3,5
3
2,5
2
1,5
1
0,5
0
1976
1980
1984
1988
1992
1996
2000
2004
2008
2012
2016
2020
704,2508
617,8668
542,0787

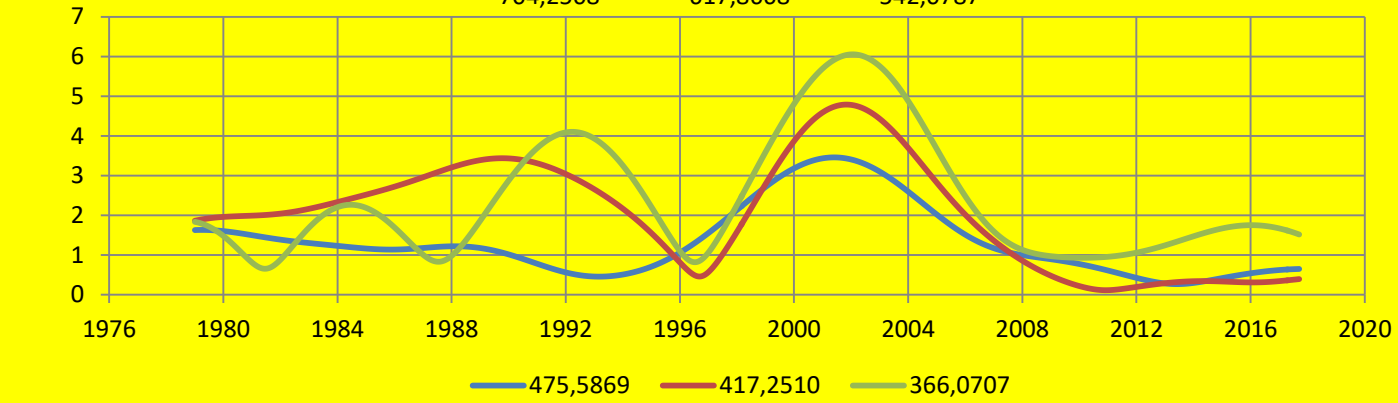
7
6
5
4
3
2
1
0
1976
1980
1984
1988
1992
1996
2000
2004
2008
2012
2016
2020
475,5869
417,2510
366,0707

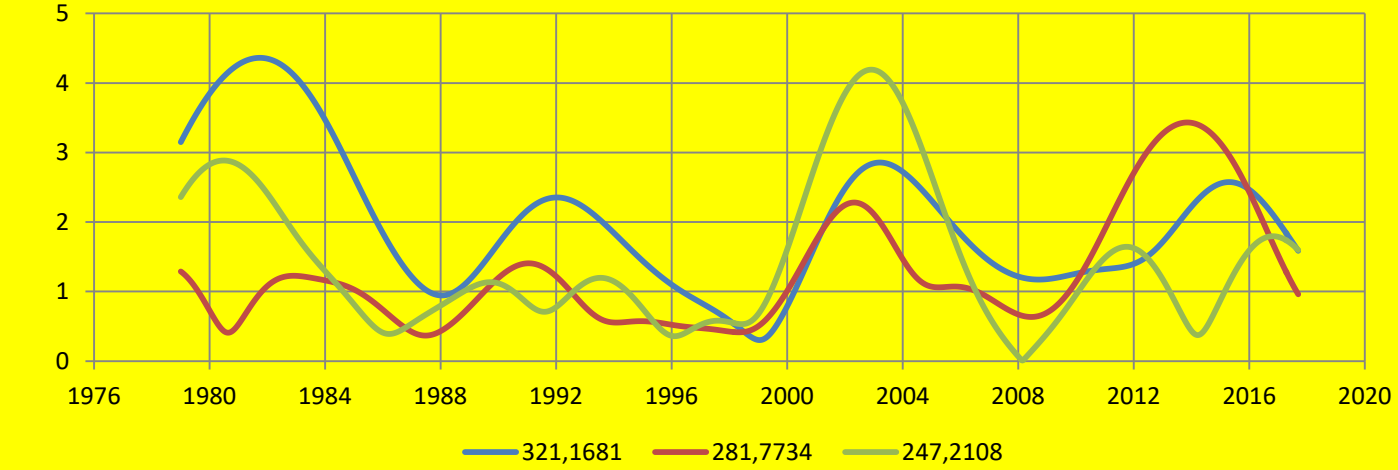
5
4
3
2
1
0
1976
1980
1984
1988
1992
1996
2000
2004
2008
2012
2016
2020
321,1681
281,7734
247,2108

Sun-Earth connections

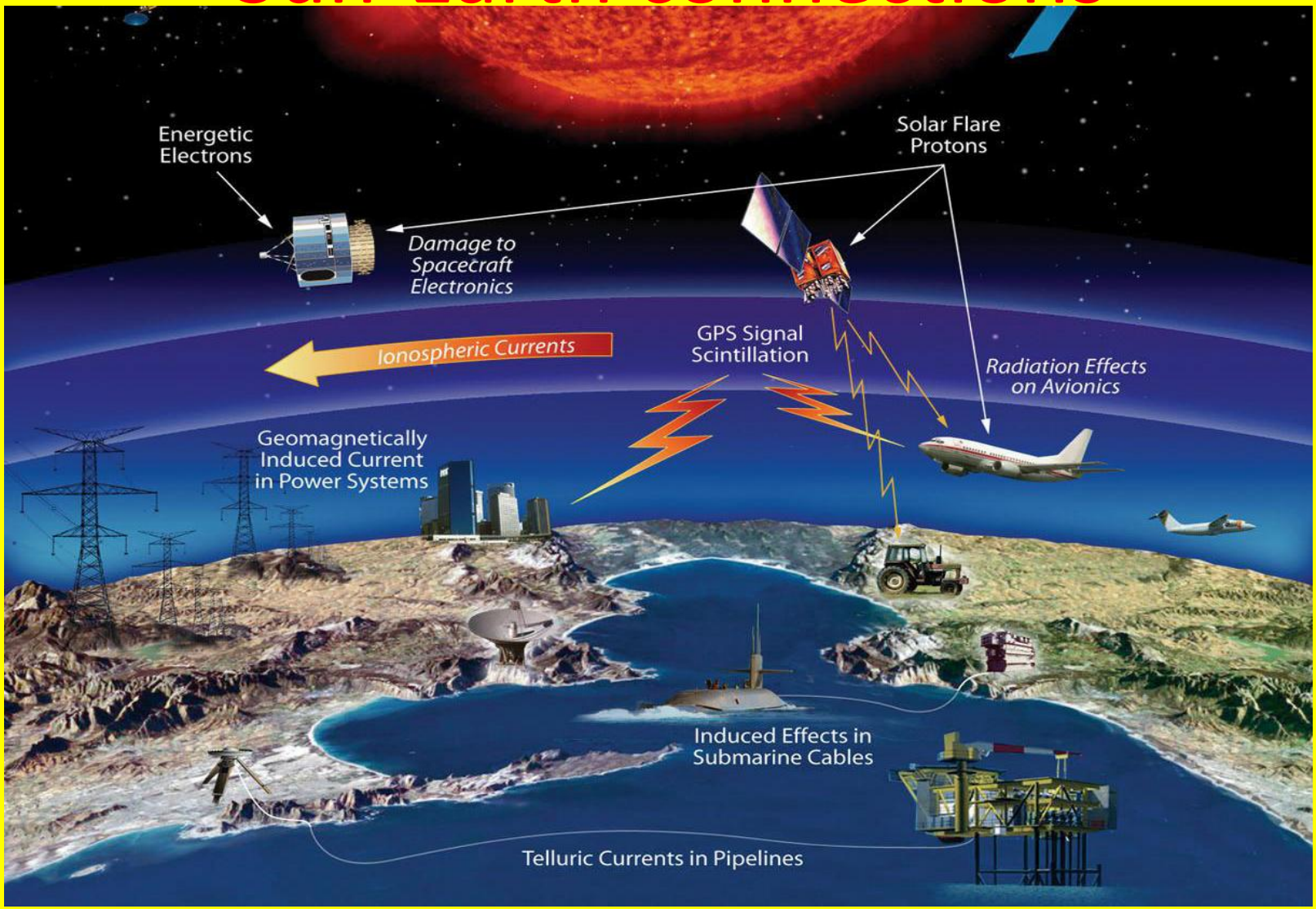

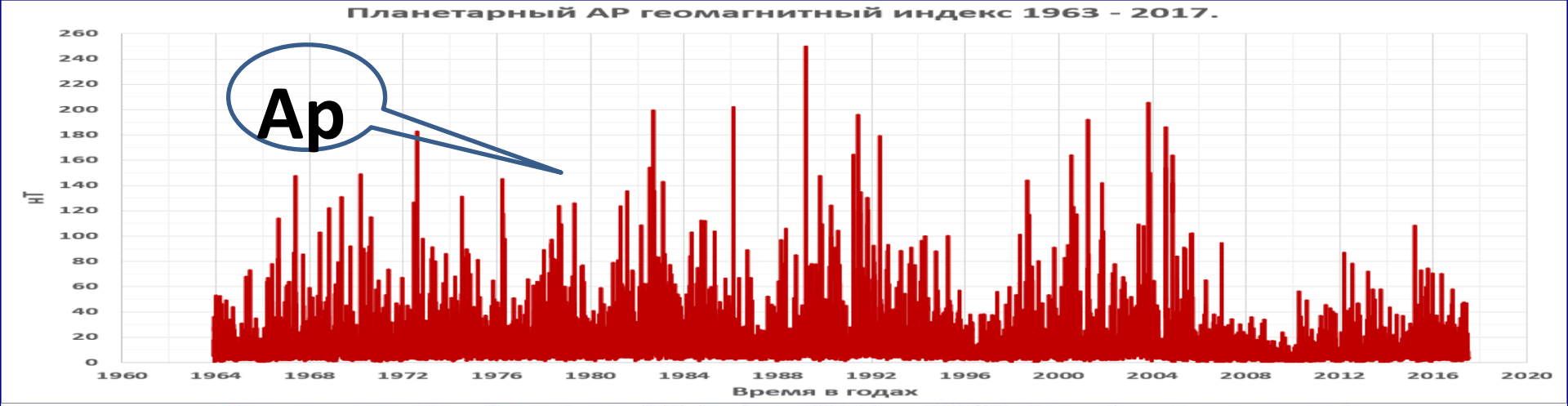
Планетарный AP геомагнитный индекс 1963 - 2017.
Ap
нТ
260
240
220
200
180
160
140
120
100
80
60
40
20
0
1960
1964
1968
1972
1976
1980
1984
1988
1992
1996
2000
2004
2008
2012
2016
2020
Время в годах

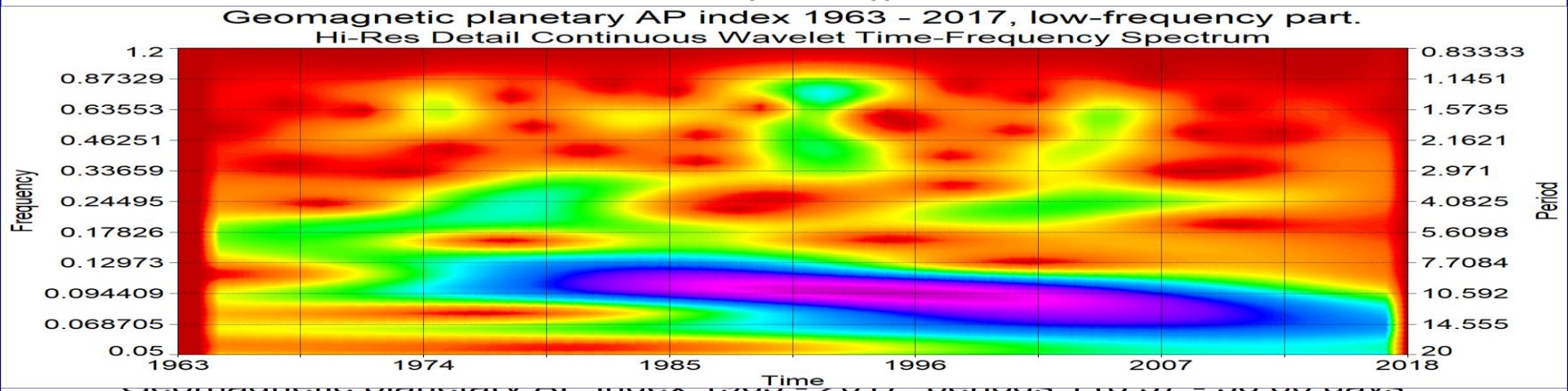
Geomagnetic planetary AP index 1963 - 2017, low-frequency part.
Hi-Res Detail Continuous Wavelet Time-Frequency Spectrum
Frequency
1.2
0.87329
0.63553
0.46251
0.33659
0.24495
0.17826
0.12973
0.094409
0.068705
0.05
Period
0.83333
1.1451
1.5735
2.1621
2.971
4.0825
5.6098
7.7084
10.592
14.555
20
1963
1974
1985
1996
2007
2018
Time

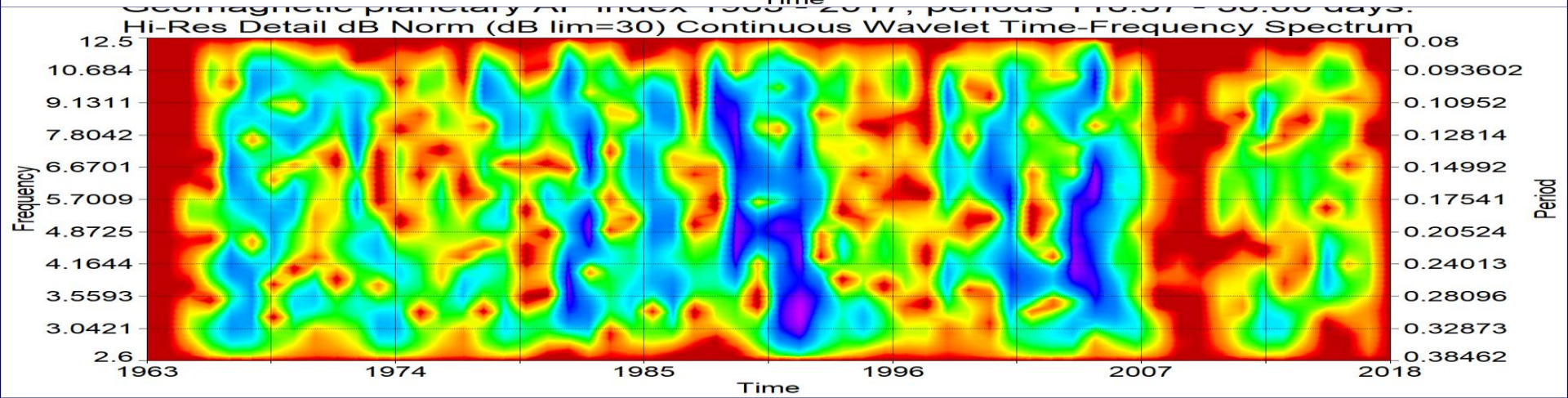
Hi-Res Detail dB Norm (dB lim=30) Continuous Wavelet Time-Frequency Spectrum
Frequency
12.5
10.684
9.1311
7.8042
6.6701
5.7009
4.8725
4.1644
3.5593
3.0421
2.6
Period
0.08
0.093602
0.10952
0.12814
0.14992
0.17541
0.20524
0.24013
0.28096
0.32873
0.38462
1963
1974
1985
1996
2007
2018
Time

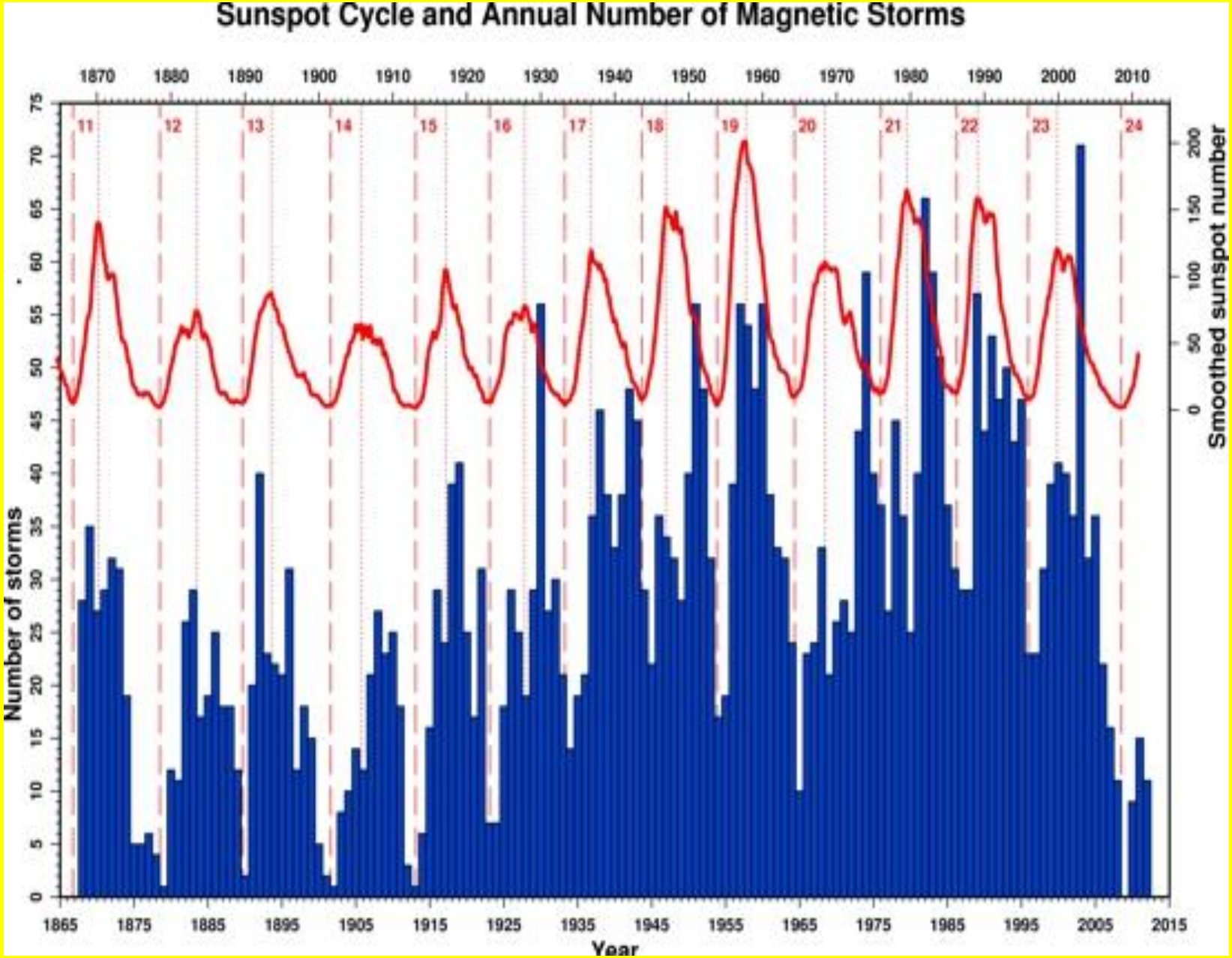
Sunspot Cycle and Annual Number of Magnetic Storms
1870
1880
1890
1900
1910
1920
1930
1940
1950
1960
1970
1980
1990
2000
2010
11
12
13
14
15
16
17
18
19
20
21
22
23
24
Number of storms
Smoothed sunspot number
1865
1875
1885
1895
1905
1915
1925
1935
1945
1955
1965
1975
1985
1995
2005
2015
Year

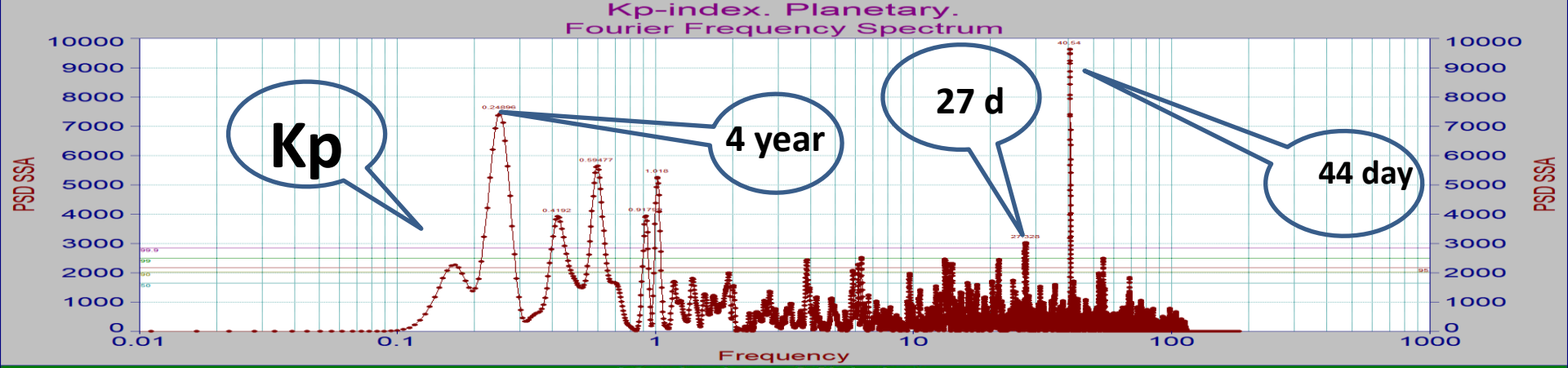
Kp-index. Planetary.
Fourier Frequency Spectrum
Kp
4 year
27 d
44 day
PSD SSA
Frequency
0.01
0.1
1
10
100
1000

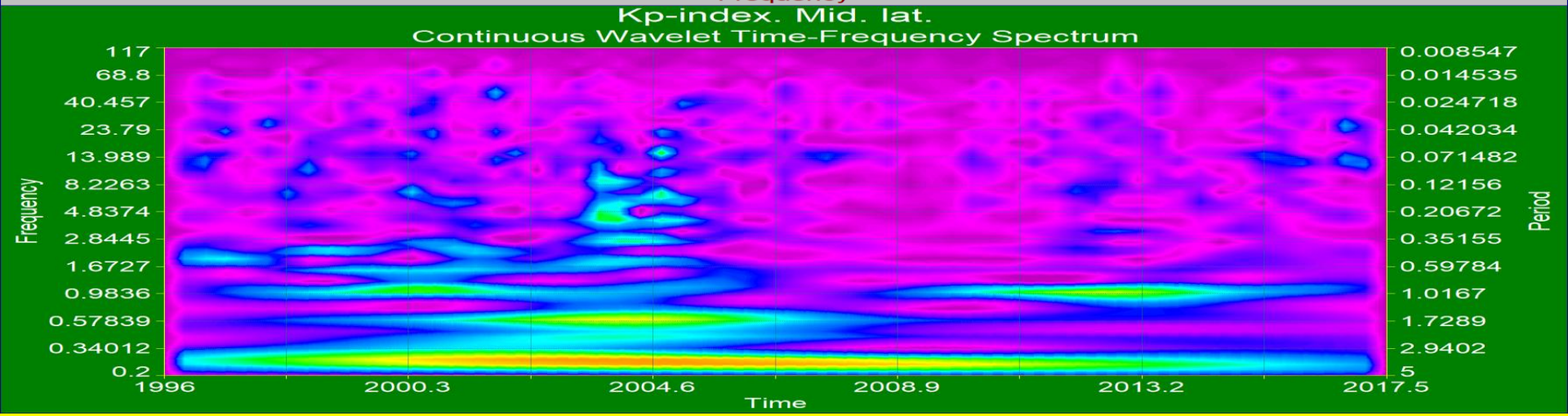
Kp-index. Mid. lat.
Continuous Wavelet Time-Frequency Spectrum
Frequency
Period
117
68.8
40.457
23.79
13.989
8.2263
4.8374
2.8445
1.6727
0.9836
0.57839
0.34012
0.2
0.008547
0.014535
0.024718
0.042034
0.071482
0.12156
0.20672
0.35155
0.59784
1.0167
1.7289
2.9402
5
1996
2000.3
2004.6
2008.9
2013.2
2017.5
Time

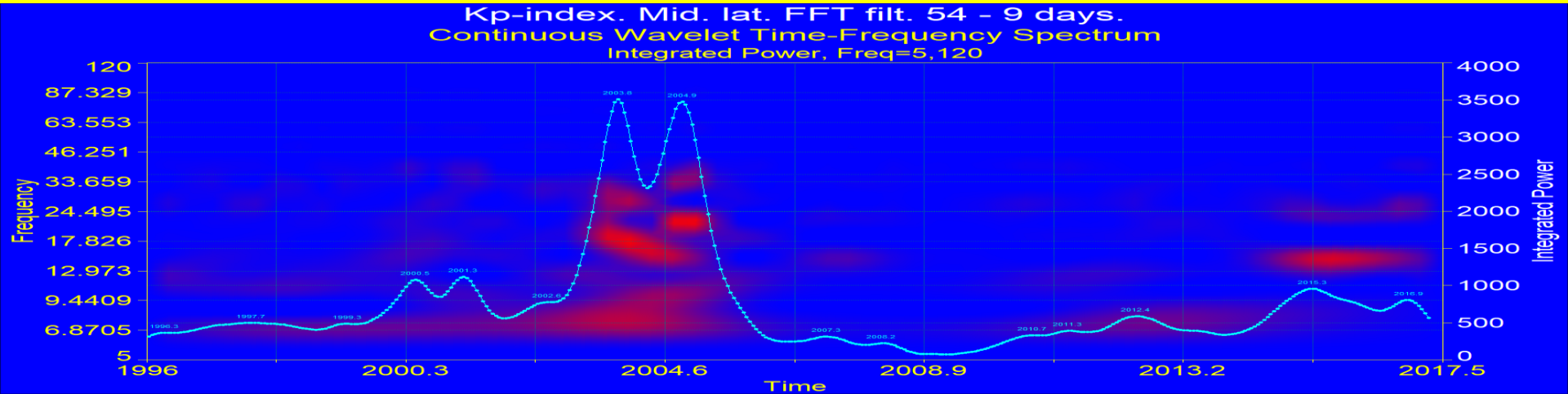
Kp-index. Mid. lat. FFT filt. 54 - 9 days.
Continuous Wavelet Time-Frequency Spectrum
Integrated Power, Freq=5,120
Frequency
Integrated Power
120
87.329
63.553
46.251
33.659
24.495
17.826
12.973
9.4409
6.8705
5
4000
3500
3000
2500
2000
1500
1000
500
0
1996
2000.3
2004.6
2008.9
2013.2
2017.5
Time

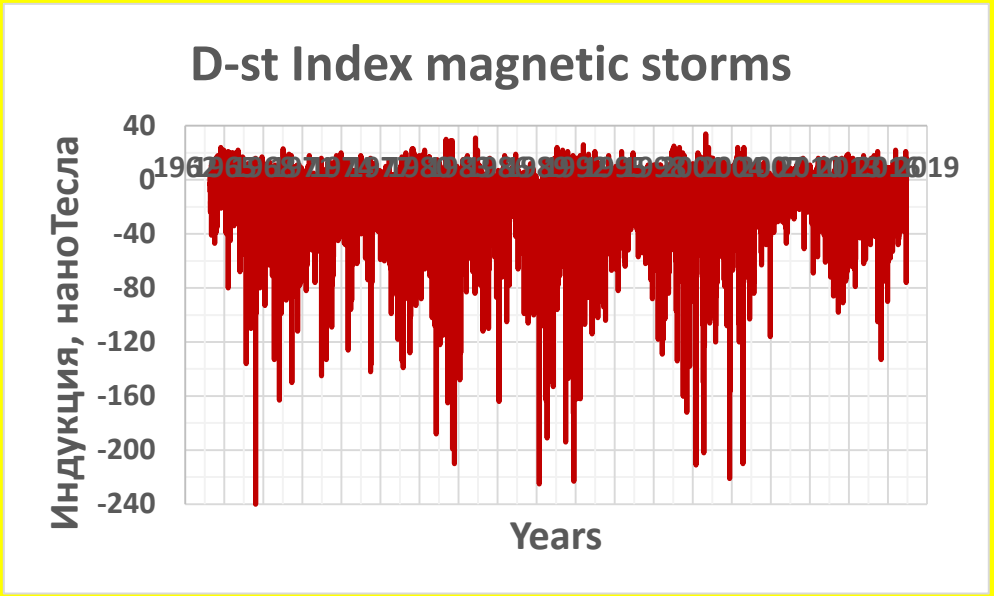
D-st Index magnetic storms
Индукция, наноТесла
40
0
-40
-80
-120
-160
-200
-240
Years

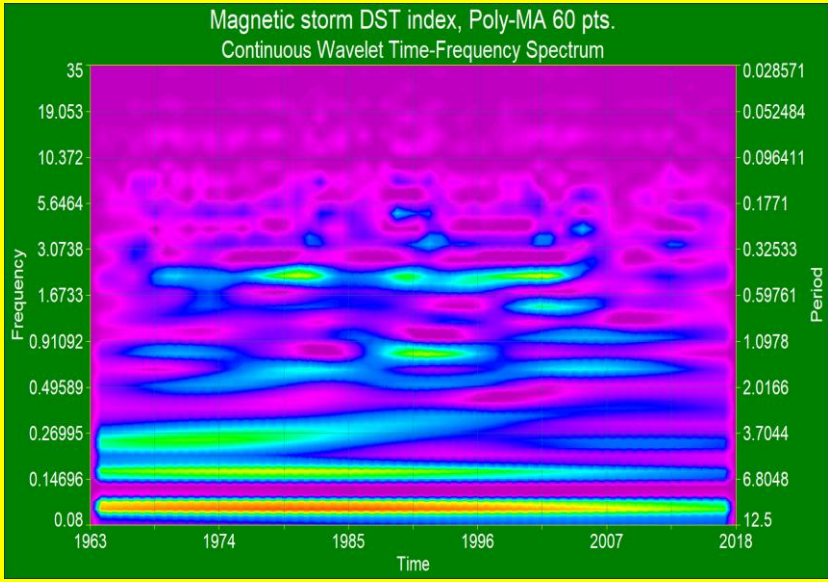
Magnetic storm DST index, Poly-MA 60 pts.
Continuous Wavelet Time-Frequency Spectrum
Frequency
35
19.053
10.372
5.6464
3.0738
1.6733
0.91092
0.49589
0.26995
0.14696
0.08
Period
0.028571
0.052484
0.096411
0.1771
0.32533
0.59761
1.0978
2.0166
3.7044
6.8048
12.5
1963
1974
1985
1996
2007
2018
Time

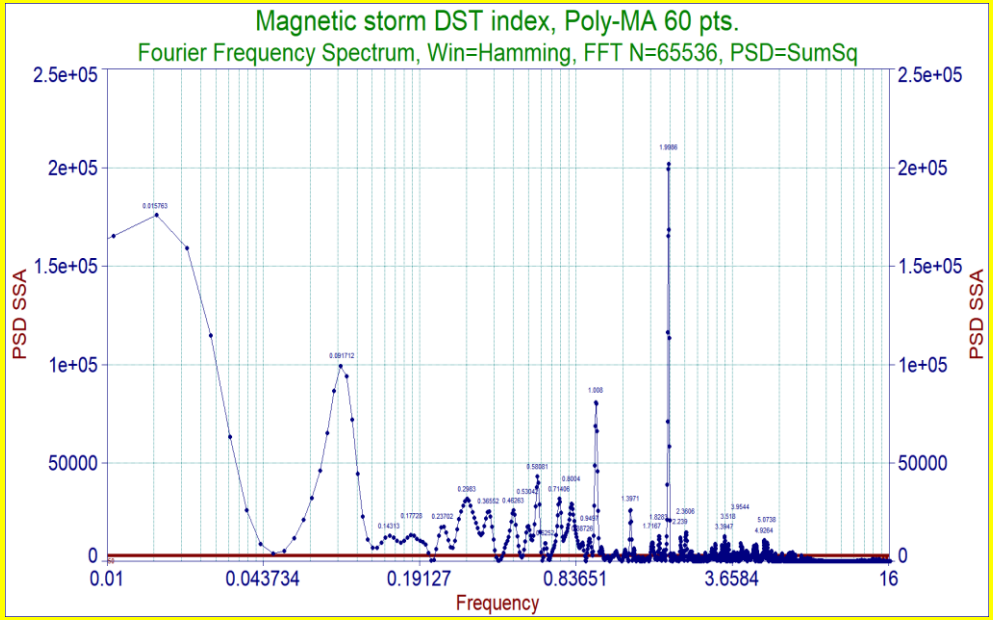
Magnetic storm DST index, Poly-MA 60 pts.
Fourier Frequency Spectrum, Win=Hamming, FFT N=65536, PSD=SumSq
PSD SSA
2.5e+05
2e+05
1.5e+05
1e+05
50000
0
0.01
0.043734
0.19127
0.83651
3.6584
16
Frequency

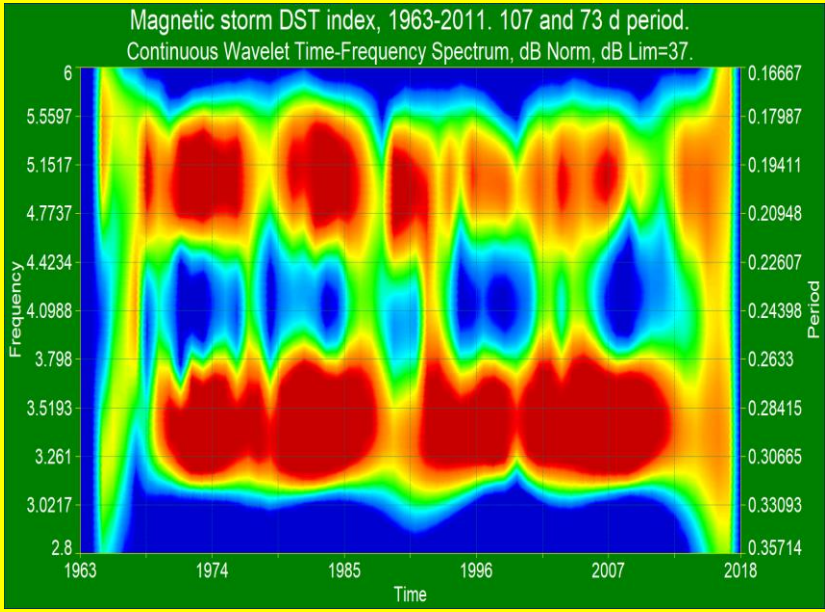
Magnetic storm DST index, 1963-2011. 107 and 73 d period.
Continuous Wavelet Time-Frequency Spectrum, dB Norm, dB Lim=37.
Frequency
6
5.5597
5.1517
4.7737
4.4234
4.0988
3.798
3.5193
3.261
3.0217
2.8
Period
0.16667
0.17987
0.19411
0.20948
0.22607
0.24398
0.2633
0.28415
0.30665
0.33093
0.35714
1963
1974
1985
1996
2007
2018
Time

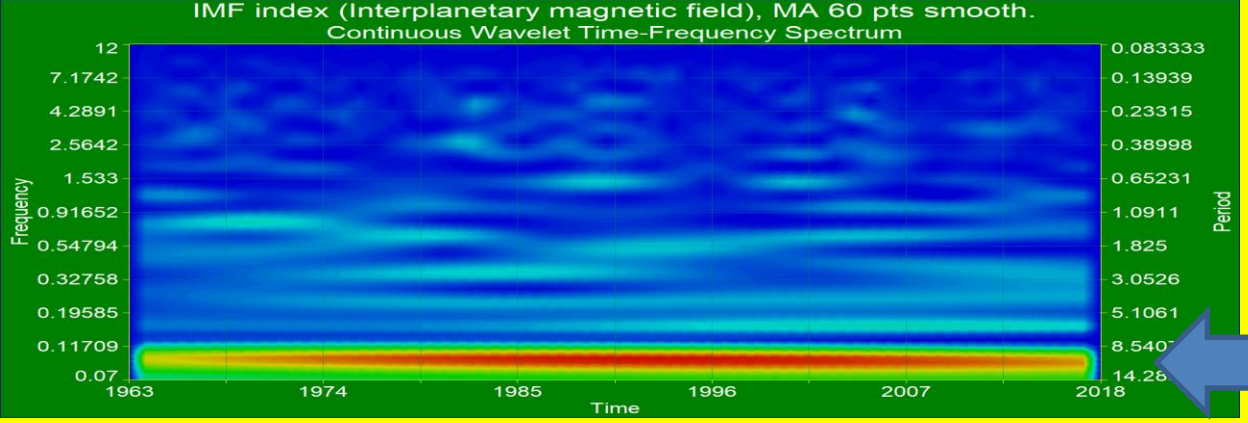

IMF index

11 –th periods

60 years

19 years

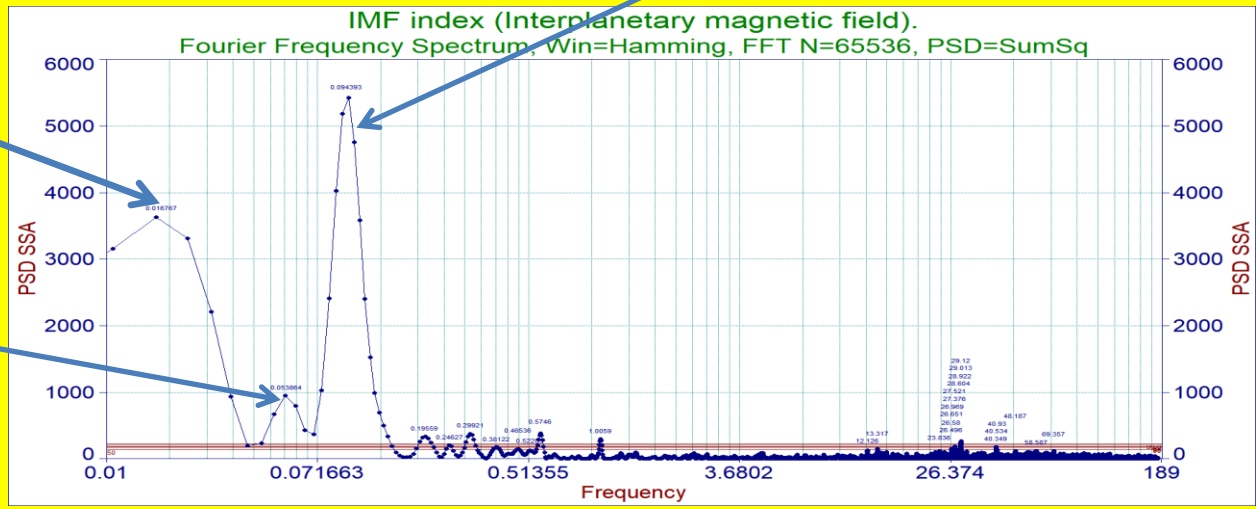

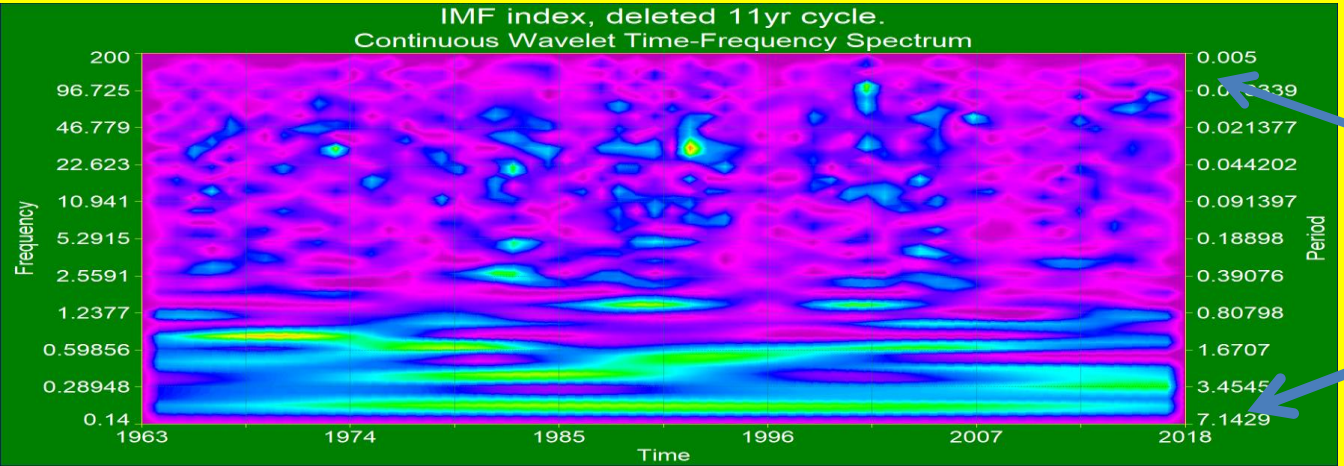

18 days-
7 years

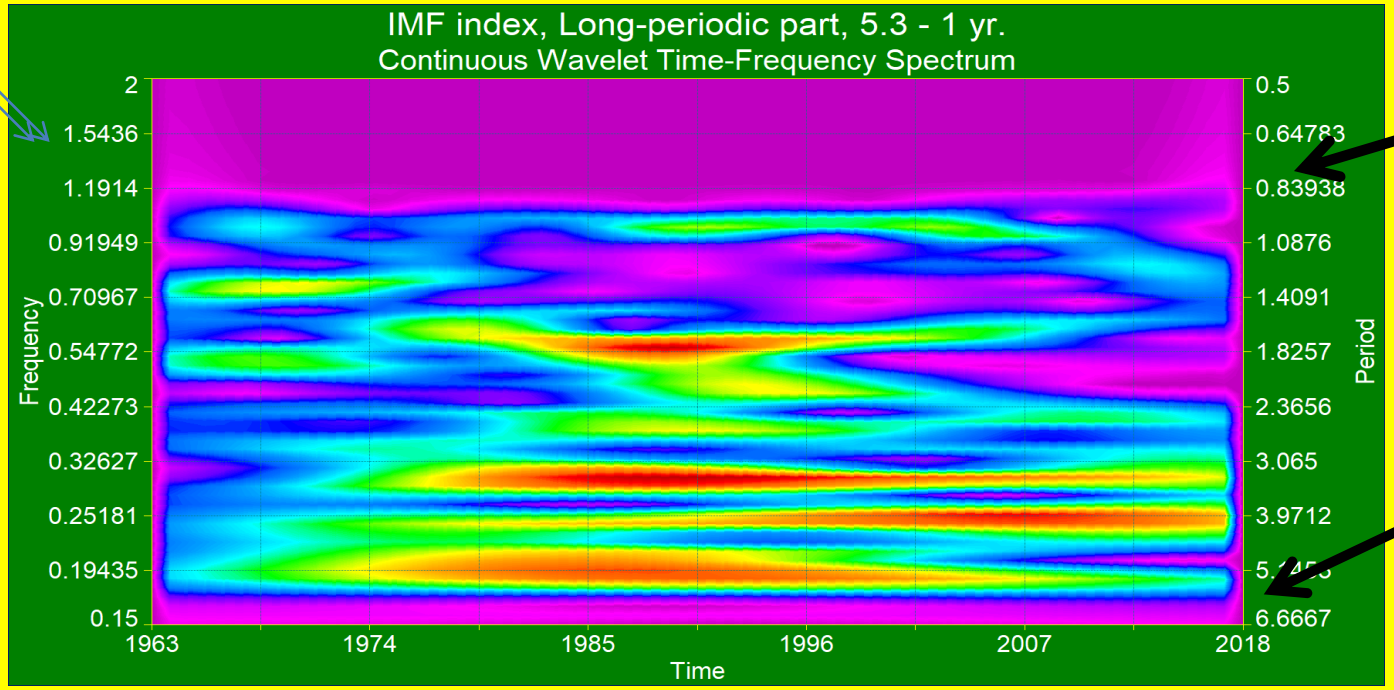

300 days

7 years

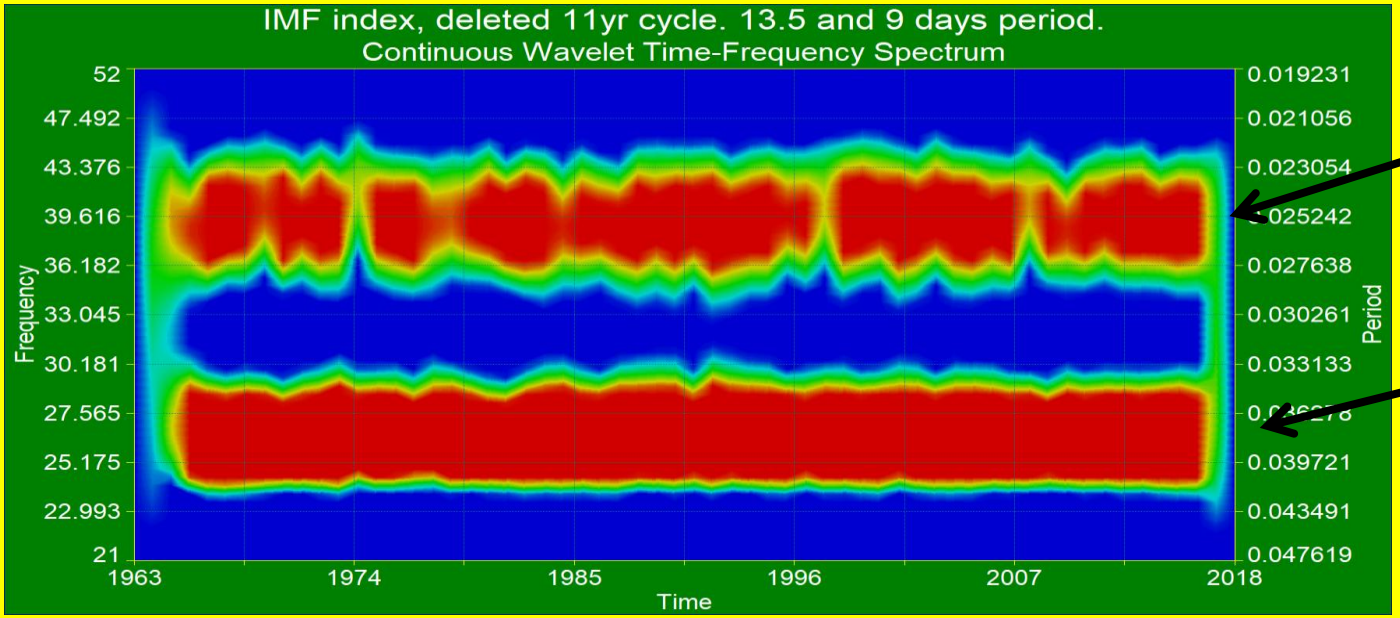

132-145 days

84 -100 days

Results

- Here there are also numerous short-term variations for a period of less than one year that change with the phase of the solar cycle.
- Changes in indices of geomagnetic activity largely reflect trends in the range of periods of solar indices.
- They demonstrate the existence of a long-period component with the transition from one cycle to another.

Results

- **Application of wavelet analysis method allows you to obtain data not only on the availability of key periods changes of the studied indexes, but also determine the time of their existence and character of amplitude change over time.**
- **The paper presents the results of the calculations of the spectra for periods of solar activity indices (Sp, W, F 10.7, FI, LA, SI), solar wind flow (IMF, density) , disturbance state of the geomagnetic field (Ap, Kp, DST). For indexes that characterize the solar activity the presence of long-period component is typical (2-7 years), which move from one cycle to another.**

Results

- **Short-periodic components exist within certain cycles of activity. Changes of the periods spectrum of solar wind indexes show numerous long-period and short-periodic components of transition from one cycle to another.**
- **Changes in solar constant (SI index) show a noticeable difference from all other solar indices showing off the most varied range of periods.**

Our research team in Radio-astronomical Institute and cooperation

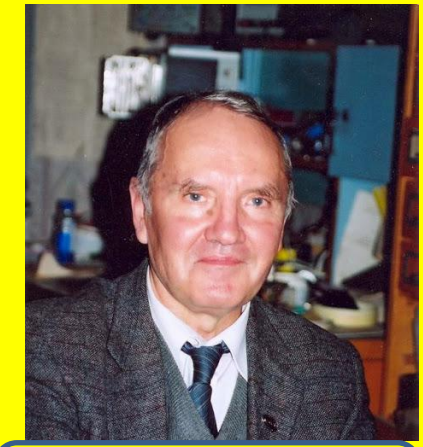

Head – Dr.Michail Ryabov

Dr. Artem Sukharev

Luba Sobitniak
Junior Staff Scientist

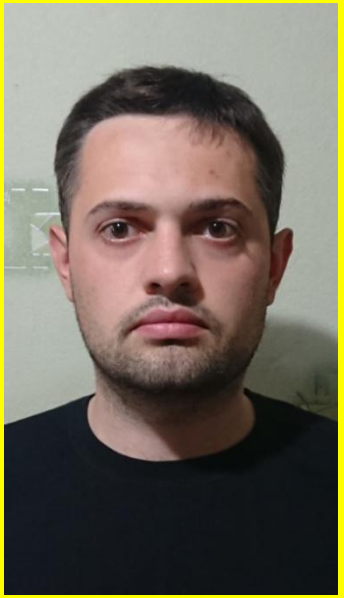

Vladimir Komendant
leading engineer-radiophysicist

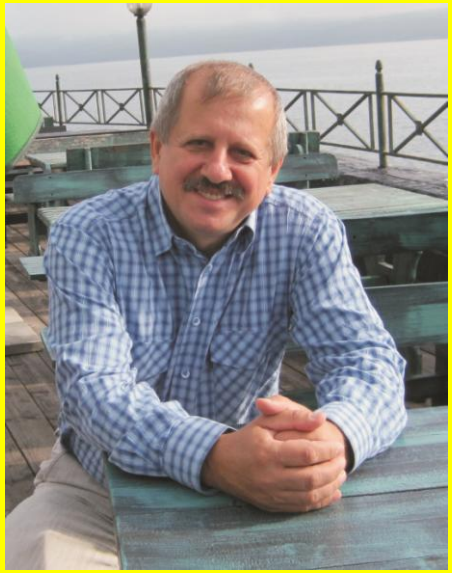

Cooperation – Prof. M.I. Orlyuk
Head Department Geomagnetic Variations Geophysics Institute NAS

[1] URAN-4 Observatory, Radio-astronomical institute of NAN of Ukraine
[2] Institute of a geophysics of NAN of Ukraine

The catalog of magnetic storms for Odessa magnetic anomaly zone, during 1987-2009 and reaction of the fluxes of powerful space radio sources in the decameter range on their development

[1]L.I. Sobitnyak,
[1]M.I. Ryabov,
[1] A.A.Pilipenko,
[1] S.K.Panishko
[2]M.I. Orlyuk

From the beginning of observations in 1987 year at a radio telescope "URAN-4" the fluxes monitoring of high-power galactic and extragalactic radio sources is carried out.

The radio telescope URAN-4 is the rectangular antenna lattice consisting of 128 broadband vibrators located in the direction the East – the West (220x22m). The size of diagram the W – E direction is equal 2,8º. Fluctuation sensitivity is 150 Jy.

Program of monitoring

3C144

- $\alpha = 05^h\ 31^m\ 30^s$ $\delta = 21^\circ\ 39^m$

3C274

- $\alpha = 12^h\ 28^m\ 18^s$ $\delta = 12^\circ\ 40^m$

3C405

- $\alpha = 19^h\ 57^m\ 47^s$ $\delta = 40^\circ\ 36^m$

3C461

- $\alpha = 23^h\ 21^m\ 07^s$ $\delta = 58^\circ\ 34^m$

- **3C144 (Crab Nebula – SNR)**

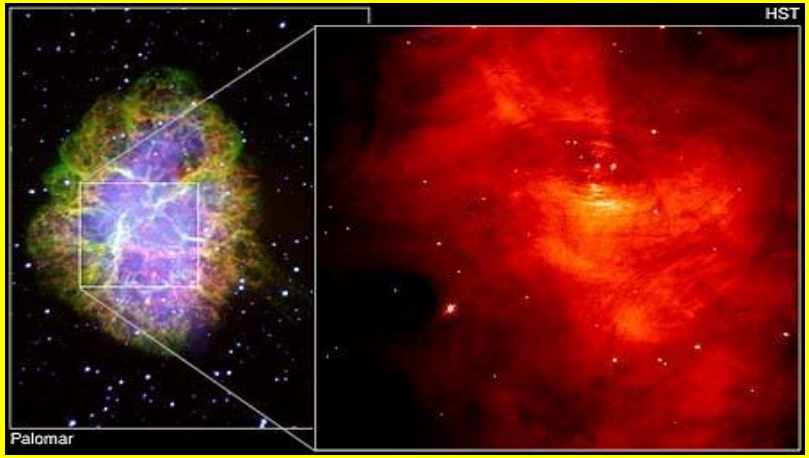

- **3C405-CygA-Radiogalaxy**

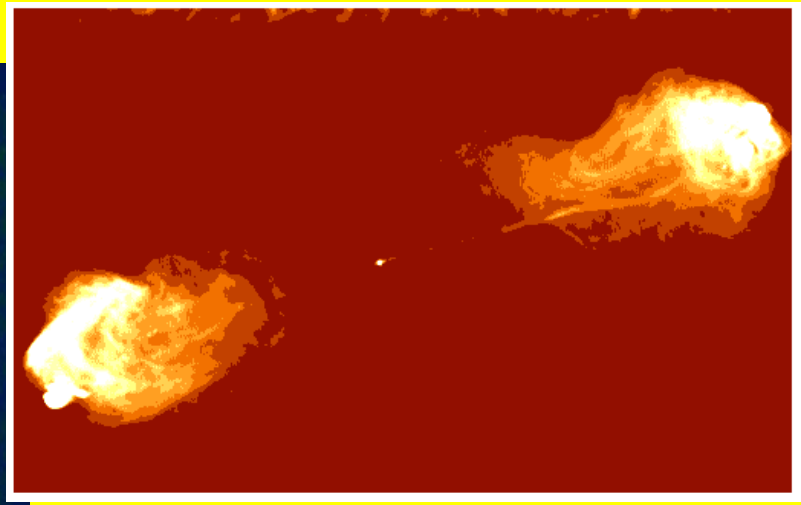

- **3C274 – VirgoA- Radiogalaxy**

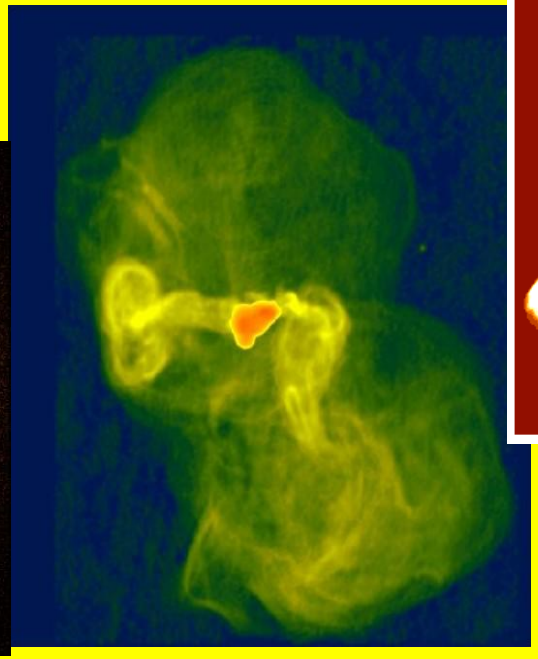

- **3C461 – CasA - SNR**

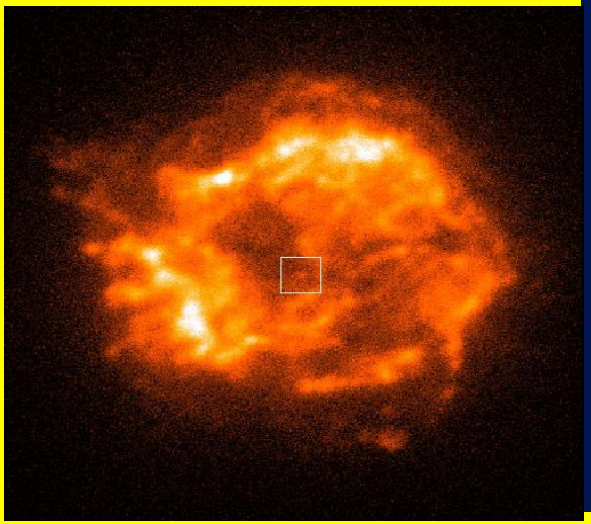

Observations of sources for 24h

3C144
-120m до + 120m , ΔT = 40m , 7 scans.

3C274
- 120m до + 120m , ΔT = 40m , 7 scans.

3C405
- 120m до + 80 m , ΔT = 40m , 6 scans.

3C461
- 60 m до + 120 m , ΔT = 60m , 4 scans

total - 13 hours 20 minutes

Exemplar of record of a source 3C405 received in the automatic registration mode

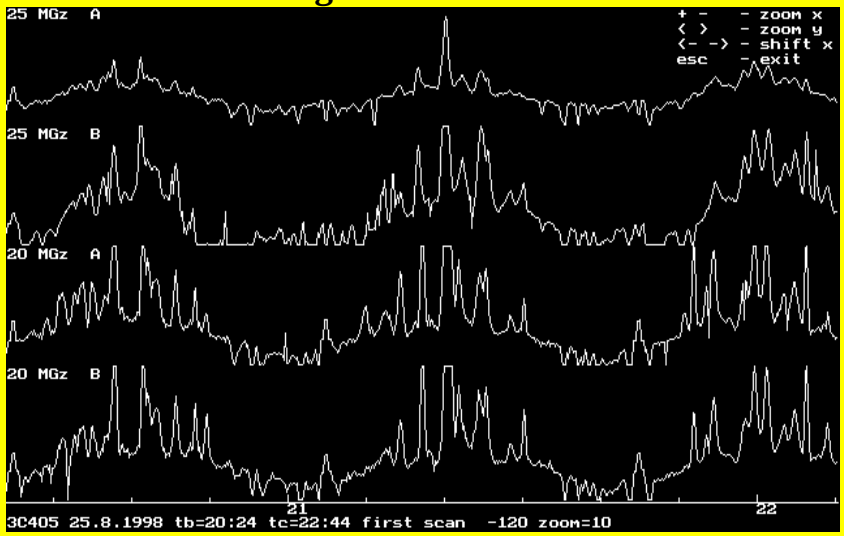

The observation time of a radiation source 3C 461

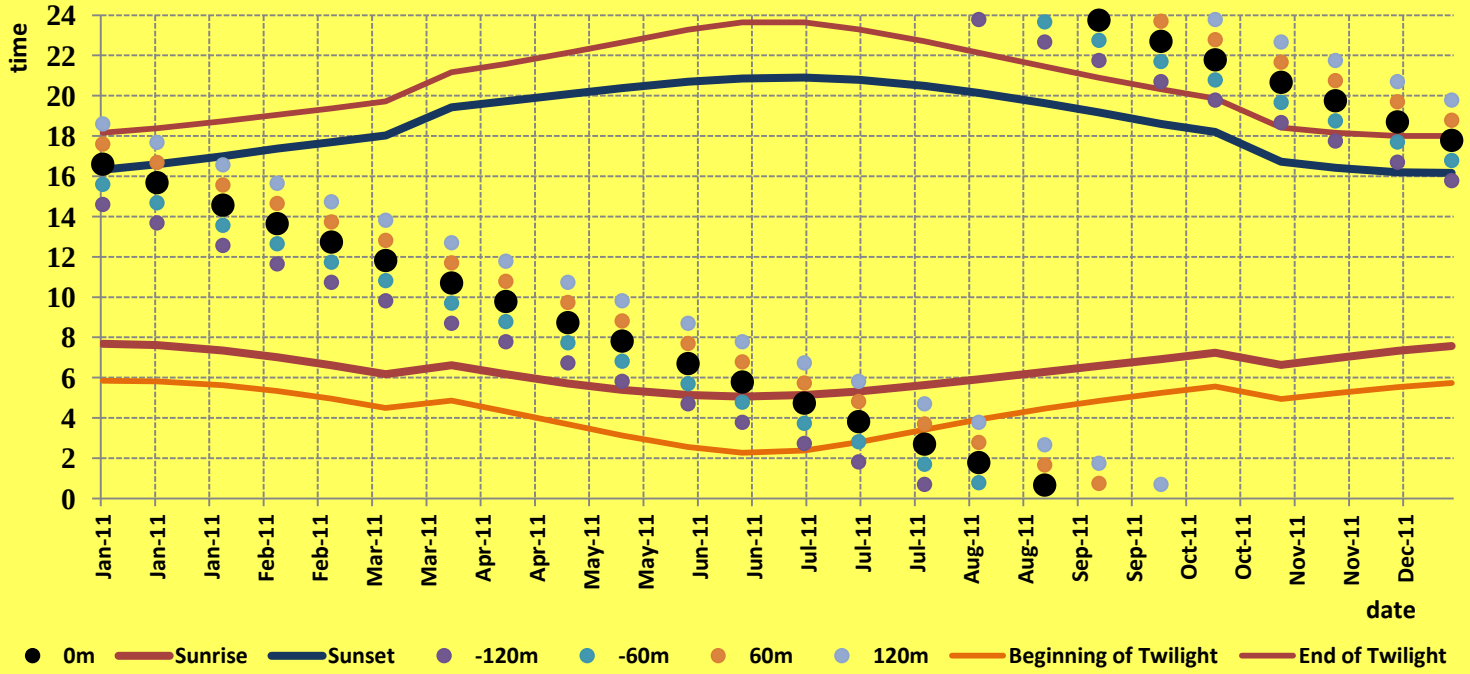

Correlative models for a radiation source 3C461 (the period - November, 2003)

Changes of a stream of a radiation source are shown by small decrease of a stream on November 3-5 and the most noticeable decrease of a stream from November 17 to November 27. During the period from November 2 to November 4 in the Sun there were 4 flashes. The most potent flash (X>17.5) happened on November 4 that entailed recession in radiation source stream level. Recession of a stream of a radiation source was not too larger as the flash happened on the edge of a solar disk and its radiation poorly affected Earth. The next period of a superactivity began since November 17. It was followed by sharp recession of level of a flux of a radiation source which continued till November 27. For three days in this fissile area eight flashes of point of M from which two were larger were made. The flash of point 2N during which there were two flashes of x-ray point of M3.2 and M3.9 was on November 18 the most interesting event of this period. Potent emission of coronal substance of this flare event caused during very larger and intensive magnetic storm on November 20-21.

3C461 radiation source flux variations on different hour corners (polarization – And, frequency – 25 MHz) in November, 2003

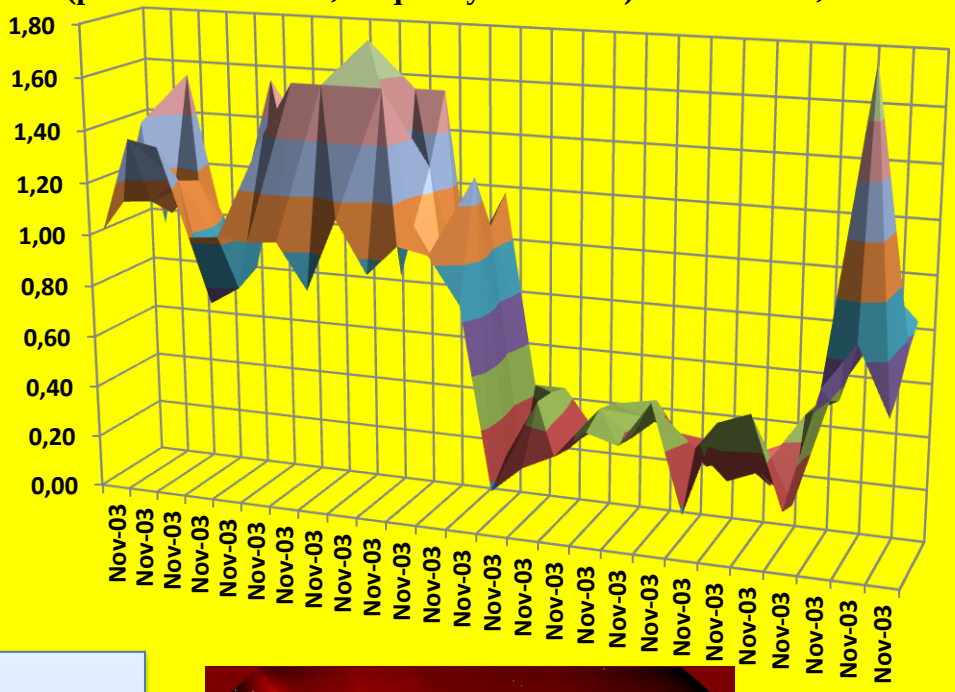

Date	Beginning UT	Duration min	Coordinates ϕ λ	Point	I_{RB}	p.f.u.	I_{ms}
02.11.03	1703	171	S14W56	X8.3/2B	R3	1540 S3	S 04.11 G2
03.11.03	0106	91	N10W83	X2.7/2B	R3		
03.11.03	0943	>36	N08W77	X3.9/2F	R3		
04.11.03	1929	80	S19W83	X>17.5 (11^m)	R5	353 S2	
05.11.03	1046	>12	S16W90	M5.3/SF	R2		
18.11.03	0716	159	N00E18	2N/M3.2/M3.9	R1		VL 20-21.11 G5
20.11.03	0735	61	N01W08	M9.6/2B	R2	10 S1	22.11 G1
20.11.03	2342	16	N00W17	M5.8/2N	R2		

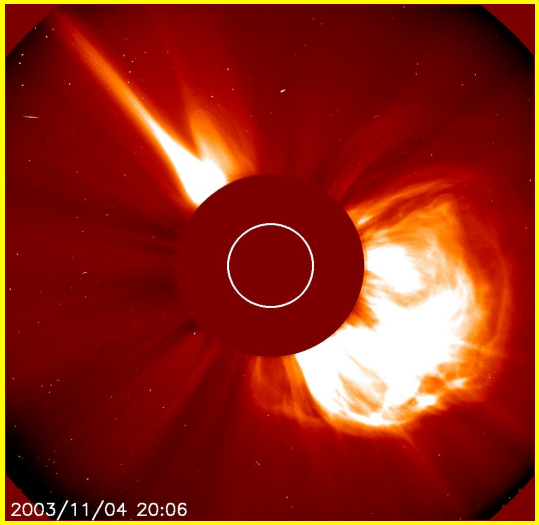

The flash which happened in the Sun on November 04, 2003

Magnetic observatory "Odessa“

The magnetic observatory "Odessa" was founded by the Novorossiysk Imperial University, in the territory of a botanical garden, at the beginning of the XX century. In 1936 it was transferred to the village of Stepanovka (near Odessa) by the Odessa State University. After world war 2th the station became to belong to the Institute of geophysics.

Since 1948 measurements of a magnetic field of Earth, with a time frame – are conducted 1 hour. At the same time measurements of three elements of a magnetic field are registered: horizontal component (H), vertical component (Z) and inducement (D).

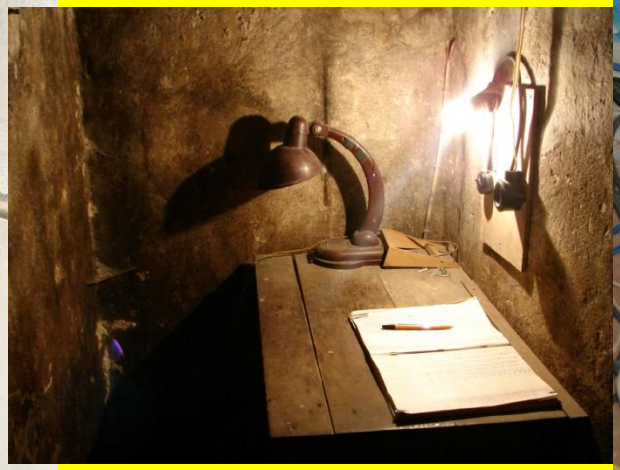

The magnetic observatory "Odessa" is situated near the intensive magnetic anomaly

The identification of the magnetic anomaly influence on geomagnetic activity comparison of characteristics of magnetic storms in Odessa and Moscow was carried out

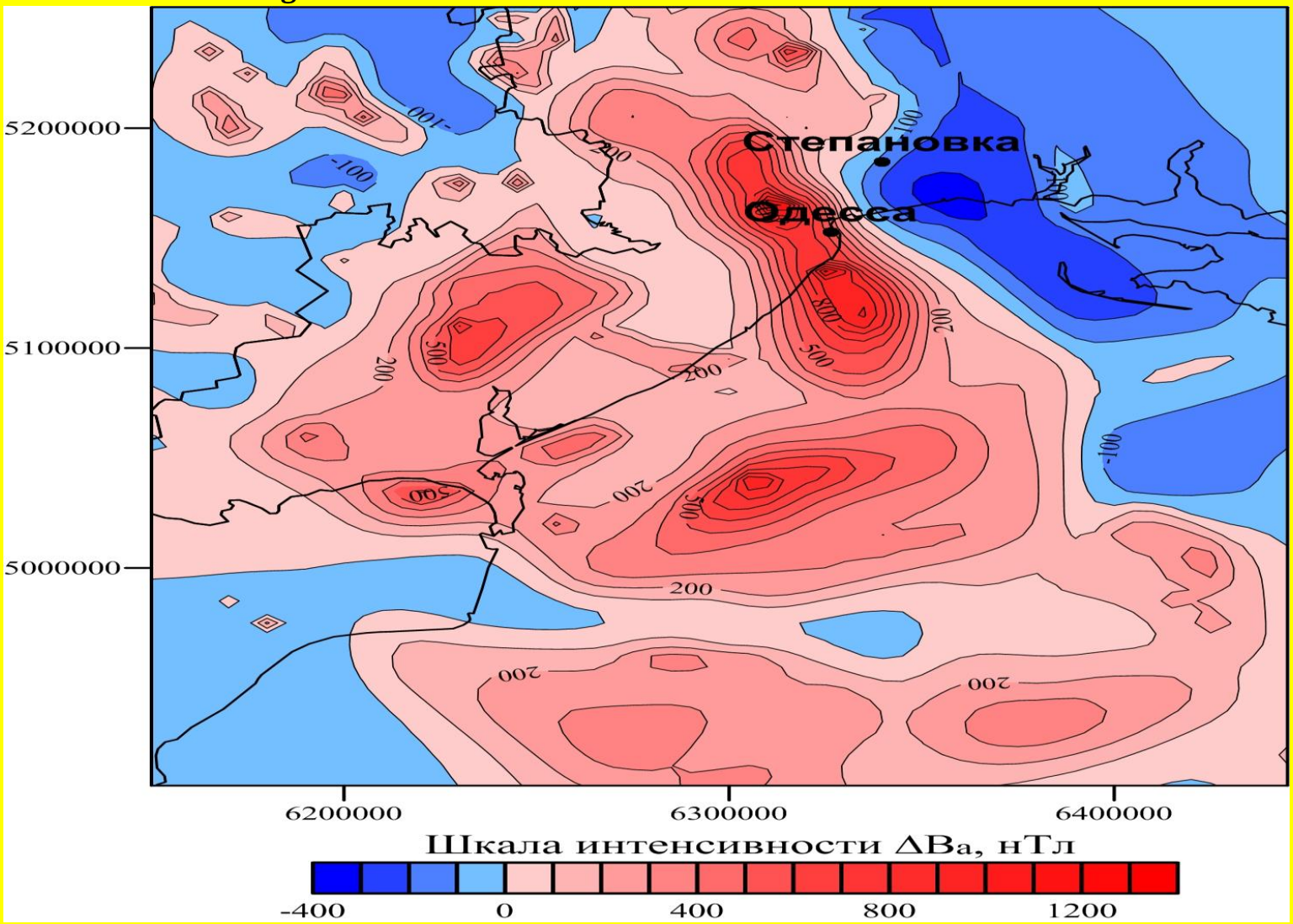

The comparison duration of the magnetic storms in Odessa and Moscow (total for the year)

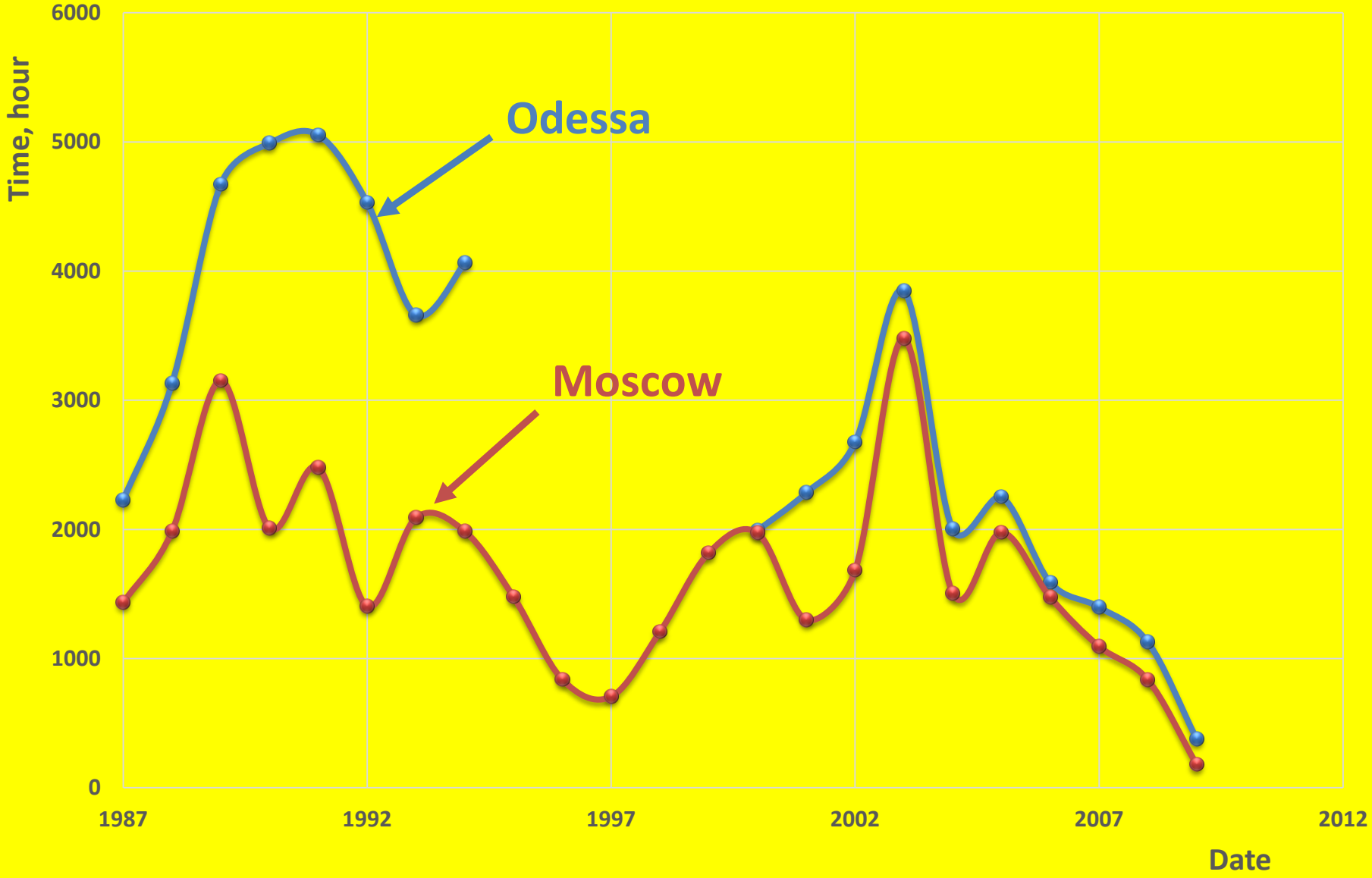

Equipment used to observation the Crab nebula radio flux rapid variability.

32-m radio telescope VIRAC, Latvia

The observations were carried out in two circular (left and right) polarizations using an uncooled 1.6 GHz reciever and SDR (Software-defined radio) total power detector with 25 MHz bandwidth as a backend.

Radio source Taurus A (3C 144).

Supernova remnant in 1054 yr. observed in China.

Multiwavelength Crab Nebula
VLA (radio) in red;
Spitzer Space Telescope (infrared) in yellow;
Hubble Space Telescope (visible) in green;
XMM-Newton (ultraviolet) in blue;
Chandra X-ray Observatory (X-ray) in purple.

The central object is the pulsar
PSR B0531 + 21 (one turn per 33 milliseconds).
Distance to nebula 6500 light years,
nebula size 11 light years, mass 4.6 solar.
Extension speed 1500 kilometers per second.

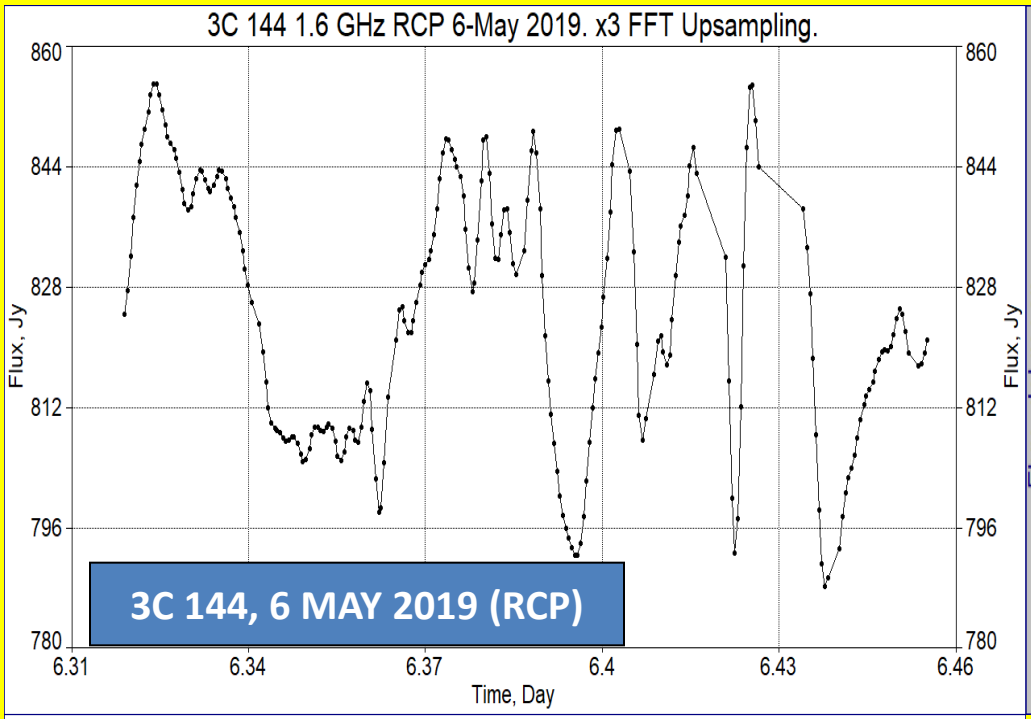

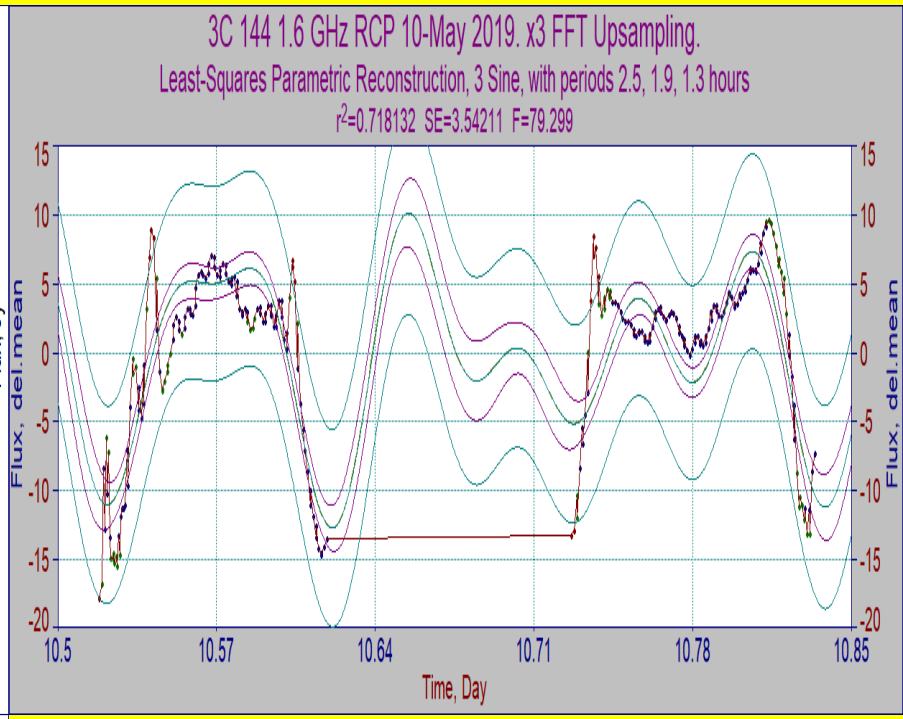

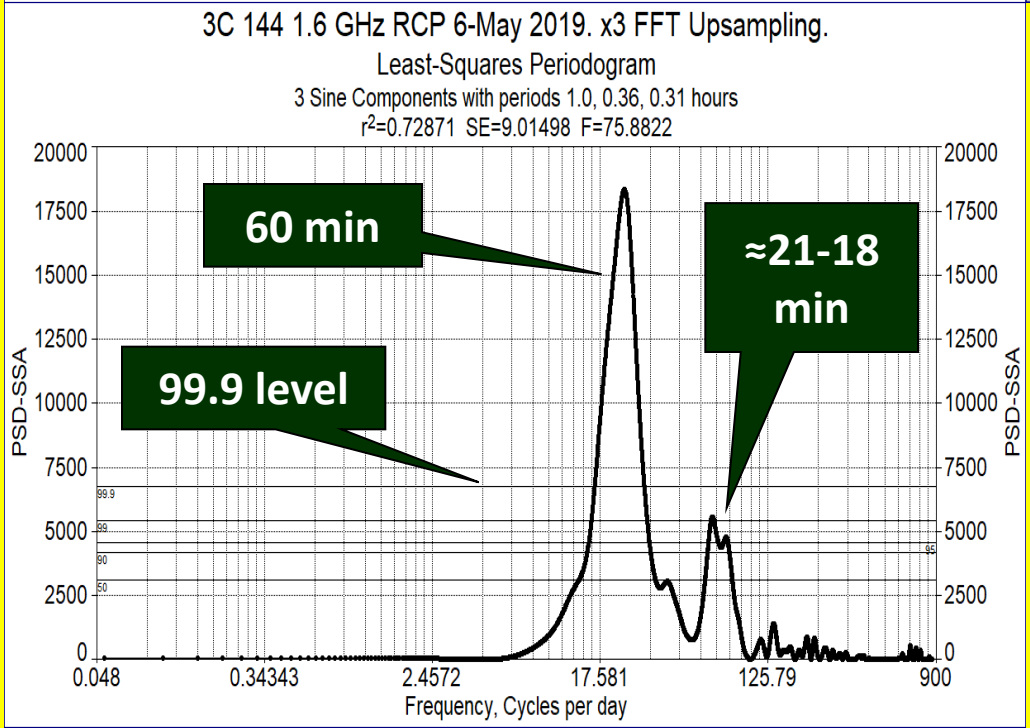

3C 144, 10 MAY 2019 (RCP), approximation by three sinusoids with periods 2.5, 1.9, 1.3 hours

On days with small number of observations, interpolation was applied (Zero-Insertion Upsampling via FFT).

In May, increased geomagnetic activity was in the following days: 1-2, 7, 10-11, 13-14, 29. Next, we consider flux density variations of radio sources in disturbances days

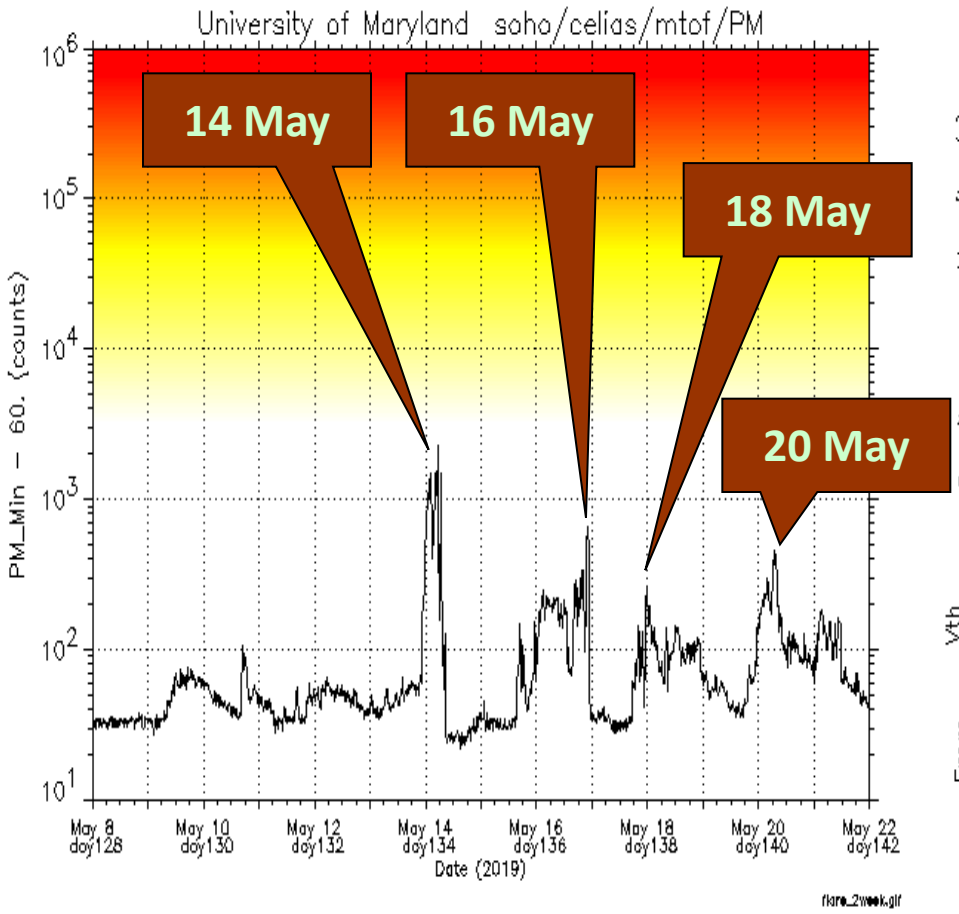

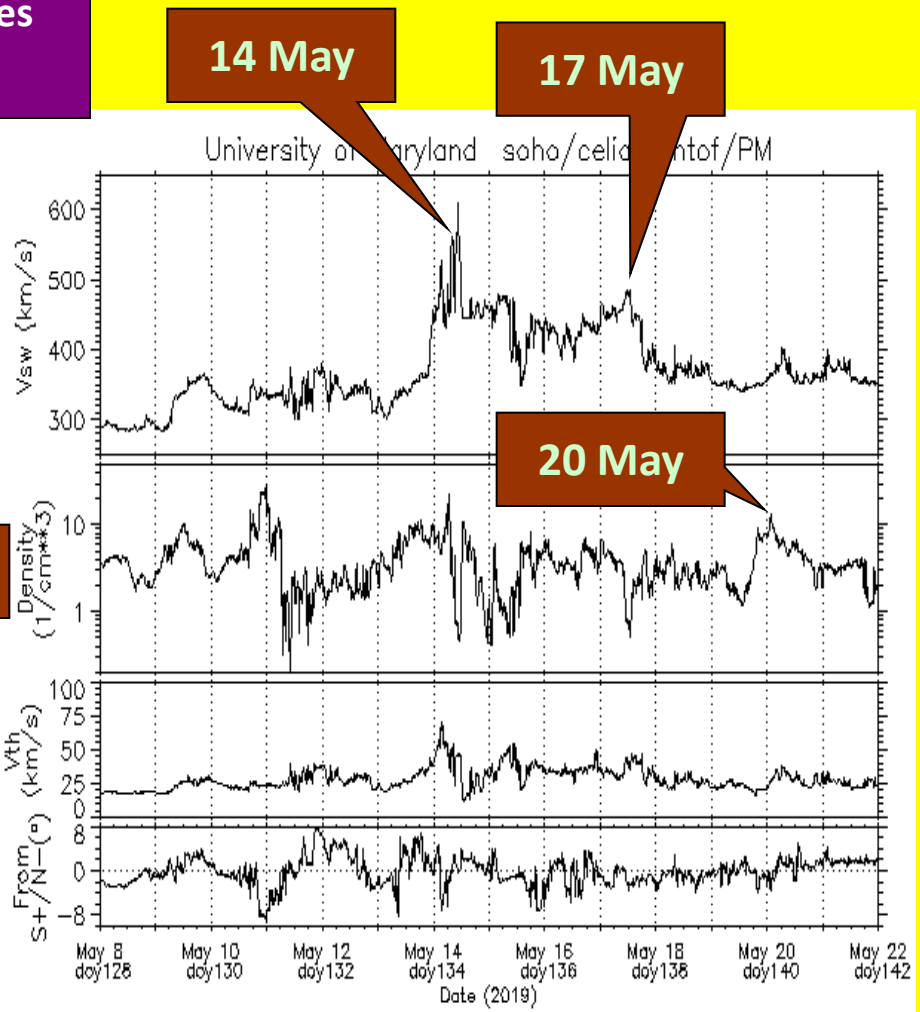

Parameters of the solar wind according to data from satellite SOHO, from Proton Monitor sensor (MAY 2019)

Data of observed objects

Two satellites with circle and elliptic orbit were taken for analysis. Serial numbers and orbital parameters (inclination and eccentricity) are shown in the tables.

satellite with circular orbit				
Number of satellite	i	e	r min	r max
00397 (2005-2017 yy)	58.3°	0.0016	613 km	621 km
satellite with elliptical orbit				
00746 (2005-2017 yy)	60.8°	0.31	399 km	6409 km

Observation data includes 13 years (2005 – 2017 yy) of observations which cover end of 23-rd and 24-th solar cycles and minimum phase between them.

In current work (to show the effects of atmospheric drag on the satellite's motion) the Bstar Drag Term is used. Observation data includes time period from March 2005 y. to September 2017 y. Values of Bstar Drag Term were obtained from NORAD data.

Example of Bstar change for satellite 00397; i=58,3°

This Drag Term includes ballistic coefficient which is a physical property of the orbiting object.[1]

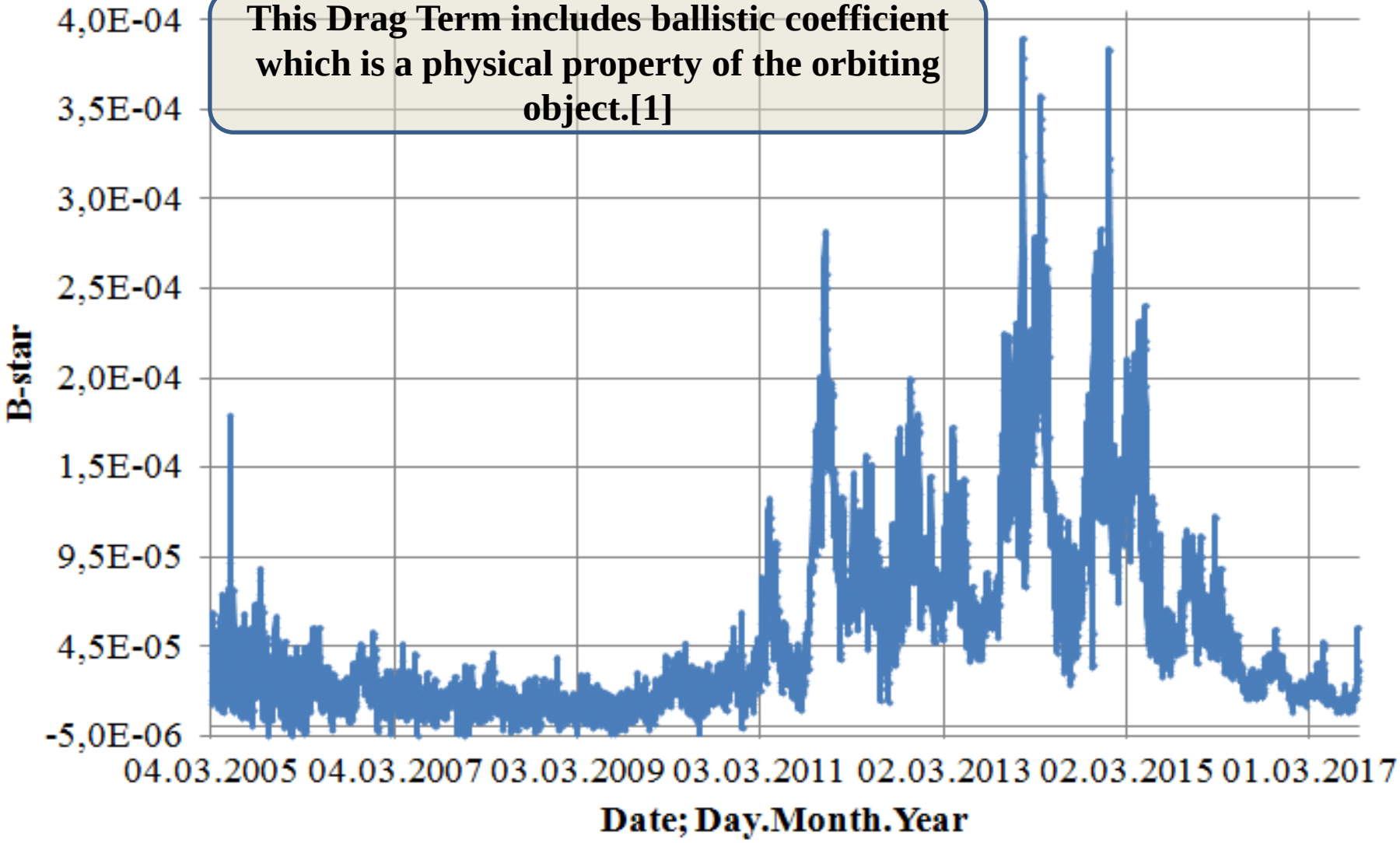

About the causes of the satellite drag for the solar and geomagnetic activity period in April 2011

	Solar Irridiance	AP	E>0,6 MeV	E>2 MeV	RadioFlux10.7cm	Sp Total	W-T	Proton density	Flow speed	Flow pressure	IMF	DST	LA
00397	0,61	0,30	0,49	0,44	-0,16	-0,66	-0,14	-0,10	0,33	0,05	0,11	-0,48	0,58
00746	0,32	0,06	0,19	0,20	-0,21	-0,57	-0,12	-0,06	0,23	0,08	-0,15	-0,28	0,23

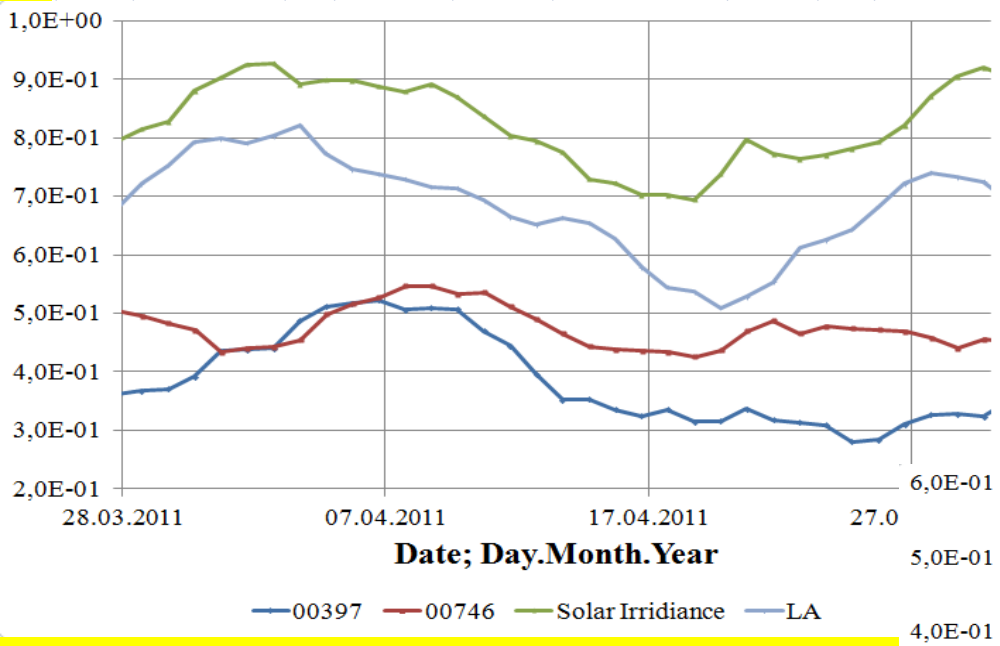

This period of satellites drag can be associated with geomagnetic disturbances caused by a coronal hole, flare activity and solar wind streams. During this period there were Earth directed flares of B and C class. They were associated with CMEs which could be geoeffective. CME directed to the south from the ecliptic plane, which could reach the Earth was detected on April 3.

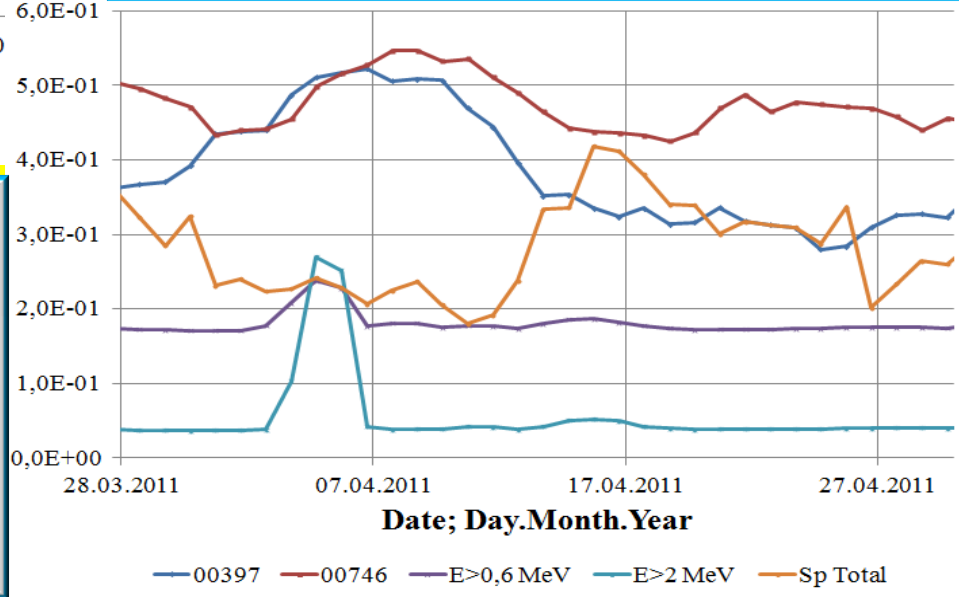

For the AES 00746, the second event is clearly visible with the beginning on April 18 and the maximum on April 21. The reason may be related to the CME, which occurred on April 15 and had a speed of 390 km / s. He reached Earth on April 18, and caused a sudden geomagnetic storm.

Thank you for your attention !